

1985

# The characteristics of sulfur trioxide formation and deposition in a pulverized-coal-fired utility boiler

Richard W. Wilson  
*Lehigh University*

Follow this and additional works at: <https://preserve.lehigh.edu/etd>

 Part of the [Chemical Engineering Commons](#)

---

## Recommended Citation

Wilson, Richard W., "The characteristics of sulfur trioxide formation and deposition in a pulverized-coal-fired utility boiler" (1985).  
*Theses and Dissertations*. 5212.  
<https://preserve.lehigh.edu/etd/5212>

This Thesis is brought to you for free and open access by Lehigh Preserve. It has been accepted for inclusion in Theses and Dissertations by an authorized administrator of Lehigh Preserve. For more information, please contact [preserve@lehigh.edu](mailto:preserve@lehigh.edu).

THE CHARACTERISTICS OF SULFUR TRIOXIDE FORMATION AND  
DEPOSITION IN A PULVERIZED-COAL-FIRED UTILITY BOILER

by

Richard W. Wilson

A Research Report

Presented to the Chemical Engineering Department

of Lehigh University in Candidacy

for the Degree of Master of Science

Lehigh University

1985

CERTIFICATE OF APPROVAL

This thesis is accepted and approved in partial fulfillment  
of the requirements for the degree of Master of Science in  
Chemical Engineering.

Dec. 26, 1985  
(Date)

Fred P. Stein  
Dr. Fred P. Stein  
(Professor in Charge)

John C. Chen  
Dr. John C. Chen  
(Department Chairman)

ACKNOWLEDGMENTS

I wish to express my sincere gratitude to the following individuals:

Professor Fred Stein for his active concern for my progress, his guidance, and the strength and enthusiasm he bestows by example.

My parents Rich and Claire, and my brothers Drew and Brian for their understanding and respect. Special recognition goes to my mother Claire, who encourages and supports my education in all circumstances, and for her suggestions, corrections, and assistance in preparing this document.

Professor Ed Levy who provided financial support for this work as Director of Lehigh's Energy Research Center through a grant from the Electric Power Research Institute.

TABLE OF CONTENTS

	<u>Page</u>
Abstract	1
1. Introduction	2
2. Flame Formation of Sulfur Trioxide	3
2.1 Flame Processes	3
2.2 The Reaction Sequence From Flame Structure	6
2.3 Association of Sulfur Dioxide and Atomic Oxygen	9
2.4 The Decomposition of Sulfur Trioxide	14
2.5 The Effect of Excess Oxygen	17
2.6 Sulfur Trioxide Formation in a Utility-Boiler Flame	19
3. Catalytic Oxidation of Sulfur Dioxide	24
4. Pulverized-Coal Combustion Characteristics	33
4.1 Conversion of Sulfur Compounds	33
4.2 Furnace Temperature Distribution	40
5. Sulfur Trioxide Measurements in a Coal-Fired Utility Boiler	46
6. Deposition Process	49
6.1 The Formation and Deposition of Sulfuric Acid	49
6.2 Ash and Liquid-Droplet Deposition	56
6.3 Acid Condensation Interference by Particles Entrained in the Gas Stream	59
6.4 Dynamics of Deposition in the Air Heater	68
Nomenclature	71
References	72

LIST OF FIGURES

<u>Figure</u>	<u>Title</u>	<u>Page</u>
1	Sulfur Trioxide Conversion Versus Residence Time	4
2	Composition Profiles of Oxygen, Sulfur Dioxide, and Sulfur Trioxide in a Flame	7
3	Effect of Reagent Concentration on Sulfur Trioxide Conversion in a Bunsen Flame	10
4	Sulfur Dioxide Oxidation in Various Bunsen Flames	11
5	Pressure Effect on Sulfur Trioxide Profiles in Hydrogen Sulfide Flames and Carbonyl Sulfide Flames	15
6	Sulfur Trioxide Profiles at Various Oxygen Levels in an Adiabatic Kerosene Furnace	18
7	Sulfur Trioxide Profiles at Various Oxygen Levels in a Non-Catalytic Furnace with Wall Cooling	20
8	Sulfur Trioxide Concentration as a Function of Oxygen Level in the Non-Catalytic Furnace with Wall Cooling	21
9	Temperature Distribution in the Non-Catalytic Furnace with Wall Cooling	22
10	Equilibrium Conversion as a Function of Temperature for the Reaction <sup>11</sup> . $\text{SO}_2 + 1/2 \text{O}_2 \rightarrow \text{SO}_3$	25
11	Catalytic Activity Development Time Dependence for a Steel Tube	26
12	Catalytic Activity Temperature Dependence for a Steel Tube	29
13	Catalytic Activity Temperature Dependence for an Iron Oxide Coated Surface	30
14	The Effect of Gas Flowrate on the Conversion of Sulfur Dioxide to Sulfur Trioxide by Catalytic Oxidation	31
15	Sequence of Physical Changes During Particle Combustion	34
16	Temperature Dependence of H <sub>2</sub> S Emission from Coal	37
17	Smoke Stack Sulfur Dioxide Emissions Versus Parent Coal Mineral Composition	39
18	Simulated Volatile Burning Time as a Function of Coal Particle Size	43

<u>Figure</u>	<u>Title</u>	<u>Page</u>
19	Char Burnout Time Versus Particle Size at 1620°K and 1420°K	44
20	Sulfur Trioxide Profiles Measured at Three Oxygen Levels in a Pulverized-Coal-Fired Utility Boiler	48
21	Equilibrium Conversion for the Reaction $SO_3 + H_2O = H_2SO_4$	50
22	Thermodynamic Dewpoint as a Function of Sulfuric Acid Concentration	52
23	Condensation Rate Versus Surface Temperature and Vapor-Dewpoint Temperature	55
24	Solid Deposition Rate Temperature Dependence	58
25	Effect of Carbon Smoke Addition on Dewpoint-Meter Conductivity-Rate Behavior Ten Degrees Centigrade Below the Instrument Dewpoint	61
26	Effect of Auxiliary Coal Firing on the Current-Rate Curve of an Stoker-Fired Utility Boiler	63
27	Effect of Auxiliary Coal Firing on the Sulfuric Acid Deposition-Rate Profile at the Duct Wall of an Stoker-Fired Utility Boiler	65
28	Effect of Ash Addition into the Flue Gas of an Oil-Fired Boiler on Dewpoint Meter Behavior	66
29	Simulated Gas-Side Air-Heater Basket Metal Temperatures (Cold End, Distributions at Inlet and Outlet)	69

LIST OF TABLES

<u>Table</u>	<u>Title</u>	<u>Page</u>
I	Coal Sulfur Classification	36
II	Composition of Condensed Liquid with Various Gas H <sub>2</sub> SO <sub>4</sub> Levels. 7.5 Percent Water Vapor 1 Atm.	53



## ABSTRACT

Parameters influencing sulfur trioxide formation in a pulverized-coal-fired utility boiler and resultant sulfuric acid deposition in the regenerative air heater were identified from literature review, analysis, and plant experimentation.

The flame reactions involved in sulfur trioxide formation and the sequence of changes which render an iron surface catalytically active towards sulfur dioxide oxidation were determined using available literature. The fundamentals were contrasted with the coal-combustion, mineral-deposition, heat-transfer, and gas-flow processes occurring in a utility boiler, in order to enumerate potential relationships between boiler operating conditions and sulfur trioxide levels. An effect of oxygen level, unit load, coal chemistry, slag condition, and coal grindsize on the flue-gas sulfur trioxide level was indicated.

Sulfur trioxide concentrations were measured as a function of oxygen level at Potomac Electric's Morgantown Unit Two, a 600-megawatt supercritical unit fired tangentially using pulverized coal. Results are included from measurements in the duct after the economizer. These measurements were made while operating at 480 megawatts using a grindsize of 85 percent through 200 mesh.

Characteristics of the binary condensation of sulfuric acid and water from a flue gas were extracted from existing information. Experimental and theoretical evidence for interference of entrained particulate material with the condensation process was recognized. The origin and nature of deposits found in regenerative-air-heater passages was related to the characteristics of the condensation process and the cycling of metal temperatures in the air-heater baskets.

## 1. INTRODUCTION

A regenerative air heater in a pulverized-coal-fired utility boiler transfers heat from the exiting flue gas to the inflowing combustion air, thereby increasing unit efficiency. The air heater contains baskets of corrugated metal sheets which rotate between the gas and air streams, absorbing heat when exposed to the exit gases while releasing heat to the combustion air. Only part of the possible reduction in exit-gas temperatures can be realized before temperatures in the air-heater passages go below the condensation temperature of the sulfuric acid in the flue gas. Under conditions where low passage temperatures support high condensation rates, metal corrosion and passage plugging from ash accumulation become intolerable. It is necessary to limit secondary heat recovery by preheating inflowing combustion air in order to maintain tolerable condensation rates.

Sulfuric acid results from the combination of sulfur trioxide and water in the product gases. The sulfur trioxide content of a flue gas is the net result of reactions in the flame region and catalytic oxidation of sulfur dioxide by active iron surfaces in the post-flame region. Sulfur trioxide and moisture concentrations dictate the acid dewpoint temperature. Condensation rates depend on acid level, fluid mechanics, and heat-transfer processes.

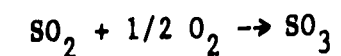
A consolidation of the factors influencing acid condensation from a flue gas and assessment of their relationship to pulverized-coal-fired utility boiler operation is necessary for planning experiments for boiler optimization. This report was developed to satisfy this need.

## 2. FLAME FORMATION OF SULFUR TRIOXIDE

### 2.1 Flame Processes

Sulfur trioxide can be formed in flames by the oxidation of sulfur compounds. Knowledge of the characteristics of this process are founded on the experimental results and analysis of Hedley.<sup>1</sup> While burning sulfur-doped kerosene in a one-dimensional controlled-mixing furnace where the flame gases completely filled the combustion chamber under fully-developed turbulent flow, gas samples were taken at various distances along the furnace. Because plug-flow conditions prevailed in the chamber, the time history of the gases was known from the gas velocity. Subsequent analysis of the gases for carbon monoxide, carbon dioxide, sulfur dioxide, and sulfur trioxide indicated the extent to which the reaction had taken place. The results for runs with 2.2 percent excess oxygen are presented in Figure 1.

A maximum in percent conversion at an intermediate time was typically observed. Gases with greater residence times possessed less sulfur trioxide, indicating sulfur trioxide decomposition. Hedley calculated the maximum theoretical yield from thermodynamic considerations for the gas reaction



at different locations along the furnace using measured values of sulfur dioxide, oxygen, and temperature. The result of this calculation appears in Figure 1 as "theoretical conversion".

The actual yield of sulfur trioxide was always greater than the theoretical maximum. Therefore, the sulfur trioxide in flames was not formed by the reaction between sulfur dioxide and molecular oxygen, because the conversion can not exceed the theoretical yield. Catalytic

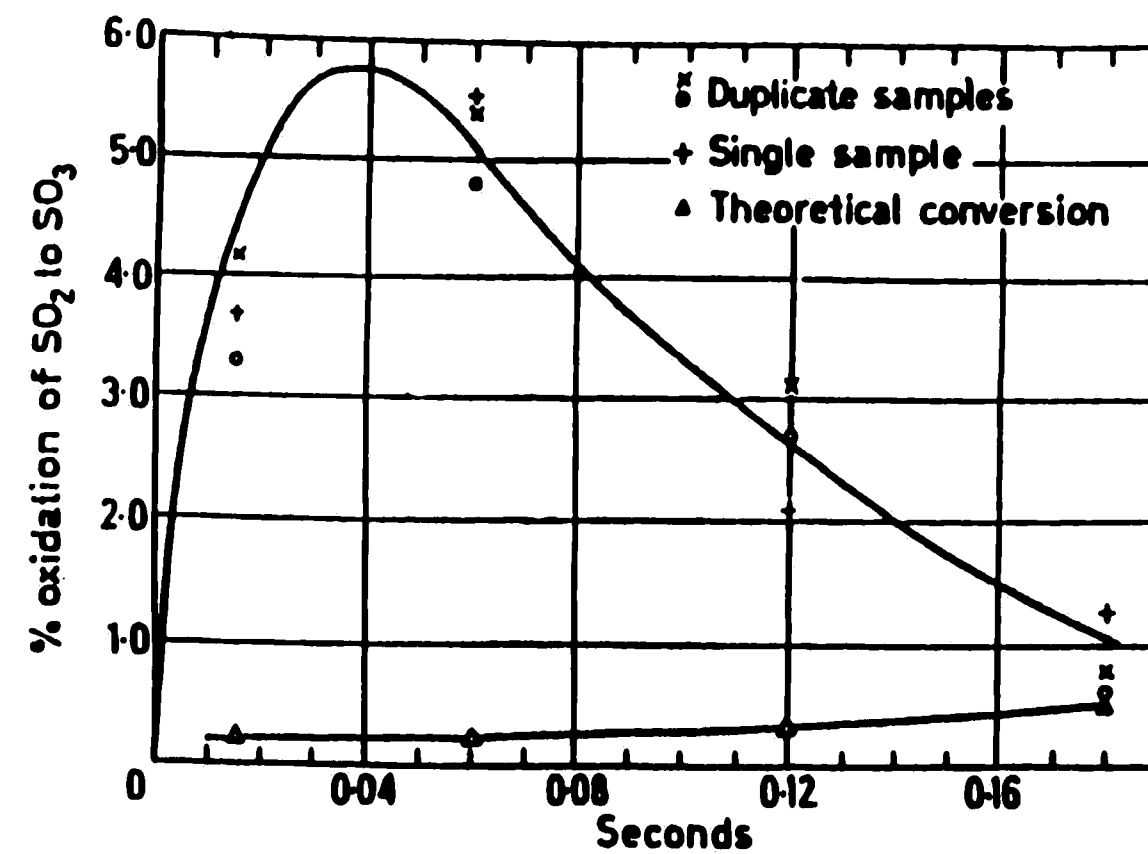
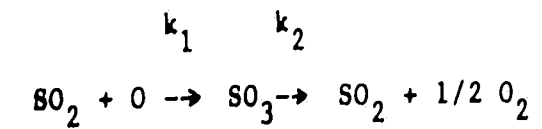


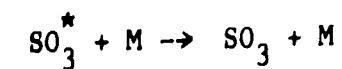
Figure 1. Sulfur Trioxide Conversion Versus Residence Time

action in the flame was ruled out because a catalyst serves only to influence the rate at which a reaction proceeds to equilibrium.

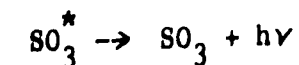
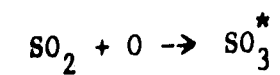
Hedley suggested an association of sulfur dioxide with atomic oxygen to form sulfur trioxide, followed by dissociation according to the consecutive reaction sequence;



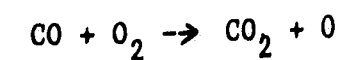
where  $k_1$  and  $k_2$  are temperature-dependent rate parameters. Sulfur dioxide is considered the precursor to sulfur trioxide because it is the only other form of sulfur in the combustion gases throughout the combustor. According to Lewis and Von Elbe,<sup>2</sup> the excess energy generated during the association of sulfur dioxide and atomic oxygen could be absorbed by a third body or by the vibrational and rotational degrees of freedom of the newly-formed molecule. In the later case, the extra energy would dissipate by either radiation or later molecular collisions.



or

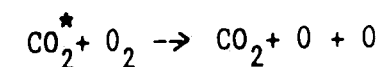
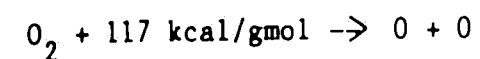


In Hedley's experiments, sulfur trioxide was not formed under fuel-rich conditions. Therefore, oxygen atoms produced in the combustion chain reactions such as



react preferentially with hydrocarbon constituents rather than sulfur

dioxide. Possible sources of atomic oxygen for sulfur dioxide oxidation include thermal decomposition of excess oxygen and dissociation of oxygen molecules by collisions with activated molecules such as carbon dioxide.

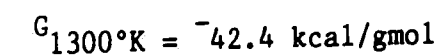
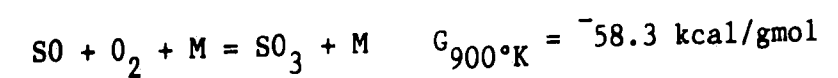


## 2.2 The Reaction Sequence From Flame Structure

Further evidence for the role of sulfur dioxide as the precursor to sulfur trioxide was found in studies of the microstructure of a sulfur-oxidizing flame. Merryman and Levy<sup>3</sup> measured concentration profiles of stable sulfur oxides in a hydrogen sulfide-oxygen flame using wet-chemistry and mass-spectrographic techniques. Results from this study are shown in Figure 2.

Sulfur trioxide was first observed early in the flame at relatively low temperatures. This pre-flame sulfur trioxide concentration reached a maximum at the flameholder, and decreased to zero at the end of the visible flame. The composition distribution in the pre-flame region was attributed to consecutive equilibrium reactions.

The first step was believed to be the association of sulfur monoxide and molecular oxygen in the presence of a third body.



Formulation of the first reaction was based on several arguments:

1. Sulfur monoxide was the only form of sulfur present preceding the appearance of sulfur trioxide.
2. The maximum sulfur monoxide concentration was observed at the

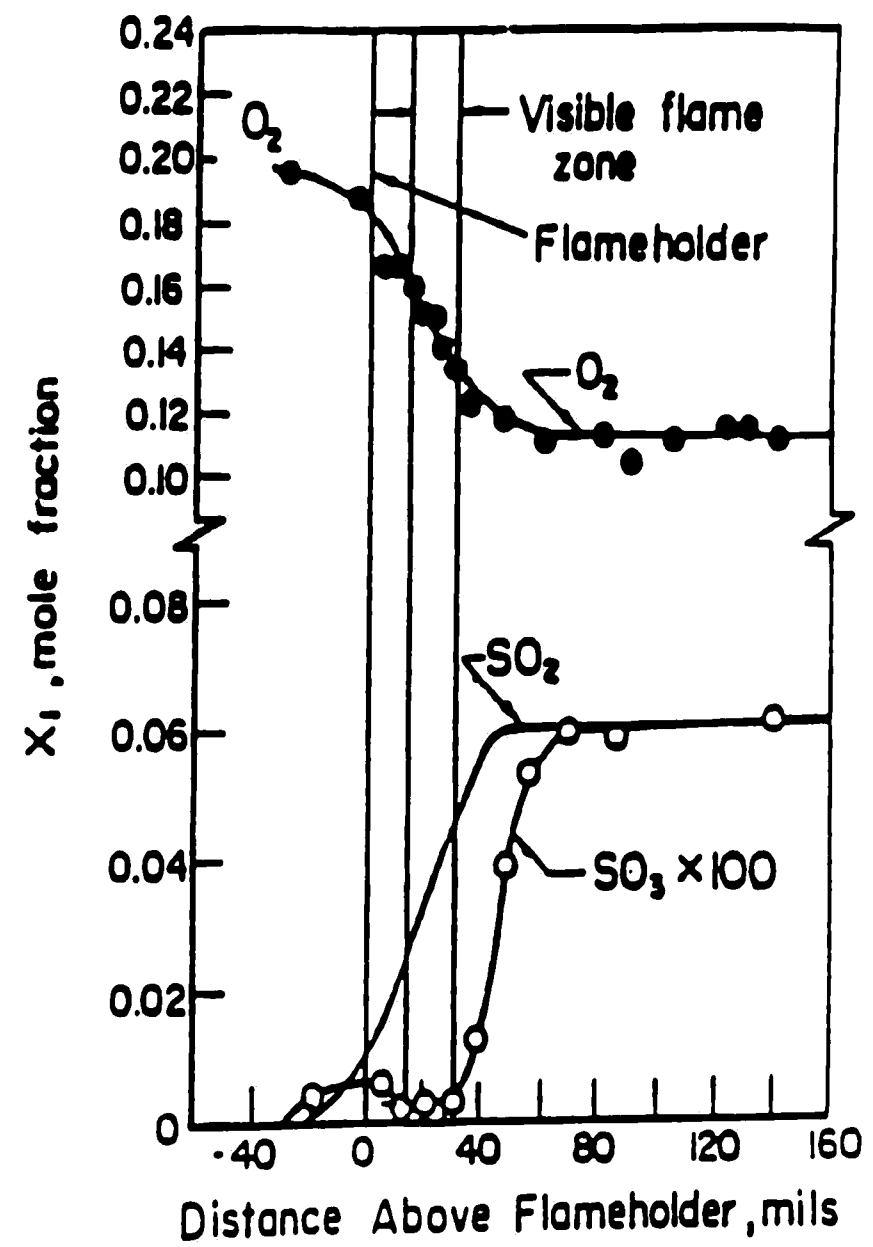
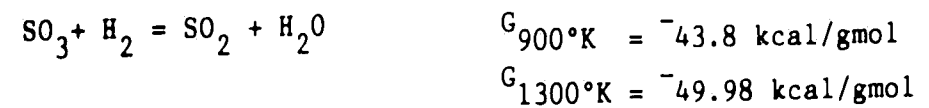


Figure 2. Composition Profiles of Oxygen, Sulfur Dioxide, and Sulfur Trioxide in a Flame

same position as maximum pre-flame sulfur trioxide, suggesting mass action through a reaction involving sulfur oxide and sulfur trioxide.

3. Sulfur monoxide is more likely in the cooler part of the flame below the flameholder because the free energy for the proposed reaction is lower there.
4. Molecular oxygen must be involved because there is no source of pre-flame atomic oxygen.
5. A third body must be involved to absorb excess association energy.

The resulting sulfur trioxide would then decompose into sulfur dioxide and water by reacting with hydrogen.



This second reaction was constructed based on the following information:

1. The sulfur trioxide concentration decreased after the flameholder, indicating decomposition.
2. Hydrogen was generated in excess by the primary flame reactions. Little sulfur trioxide was available in the region of maximum hydrogen concentration, suggesting that sulfur trioxide levels were diminished due to a reaction between sulfur trioxide and hydrogen.
3. According to the free energy of the proposed decomposition reaction, decomposition was favored at the higher temperatures of the visible-flame zone, where the lowest sulfur trioxide concentrations were observed.

Sulfur trioxide was then generated in the post-flame region and prevailed to the furnace exit. The formation of sulfur trioxide in this region was preceded by the appearance of large quantities of sulfur dioxide. Because sulfur dioxide was the only identified form of sulfur in this zone, sulfur dioxide was acting as the precursor in the

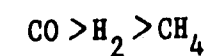


formation of sulfur trioxide. The sulfur dioxide was believed to combine with atomic oxygen due to close agreement between the calculated oxygen-atom profile and the rate of formation of sulfur trioxide.

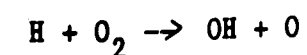
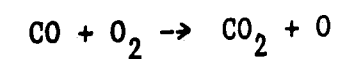
### 2.3 Association of Sulfur Dioxide and Atomic Oxygen

Dooley and Whittingham<sup>4</sup> obtained additional evidence for the association of atomic oxygen and sulfur dioxide in the post-flame region by measuring the sulfur trioxide levels in product gases from Bunsen flames which had been treated with known flame inhibitors and catalysts. Inorganic oxygen scavengers, such as carbon tetrachloride added to town-gas Bunsen flames, reduced the percent oxidation of sulfur dioxide as shown in Figure 3.

Similarly, nitric oxide added to a town-gas Bunsen flame reduced sulfur dioxide oxidation, as a result of the relative success of the reaction  $\text{NO} + \text{O} \rightarrow \text{NO}_2 + h\nu$  in competing with sulfur dioxide for atomic oxygen. In flames of carbon monoxide, hydrogen, and methane, the percent oxidation of sulfur dioxide to sulfur trioxide varied from flame to flame, following the order



as shown in Figure 4. The higher conversions in the carbon monoxide and hydrogen flames were attributed to the formation of oxygen atoms by the reactions:



In these flames, oxygen atoms were available for sulfur dioxide oxidation because hydrocarbons were not available to compete for the

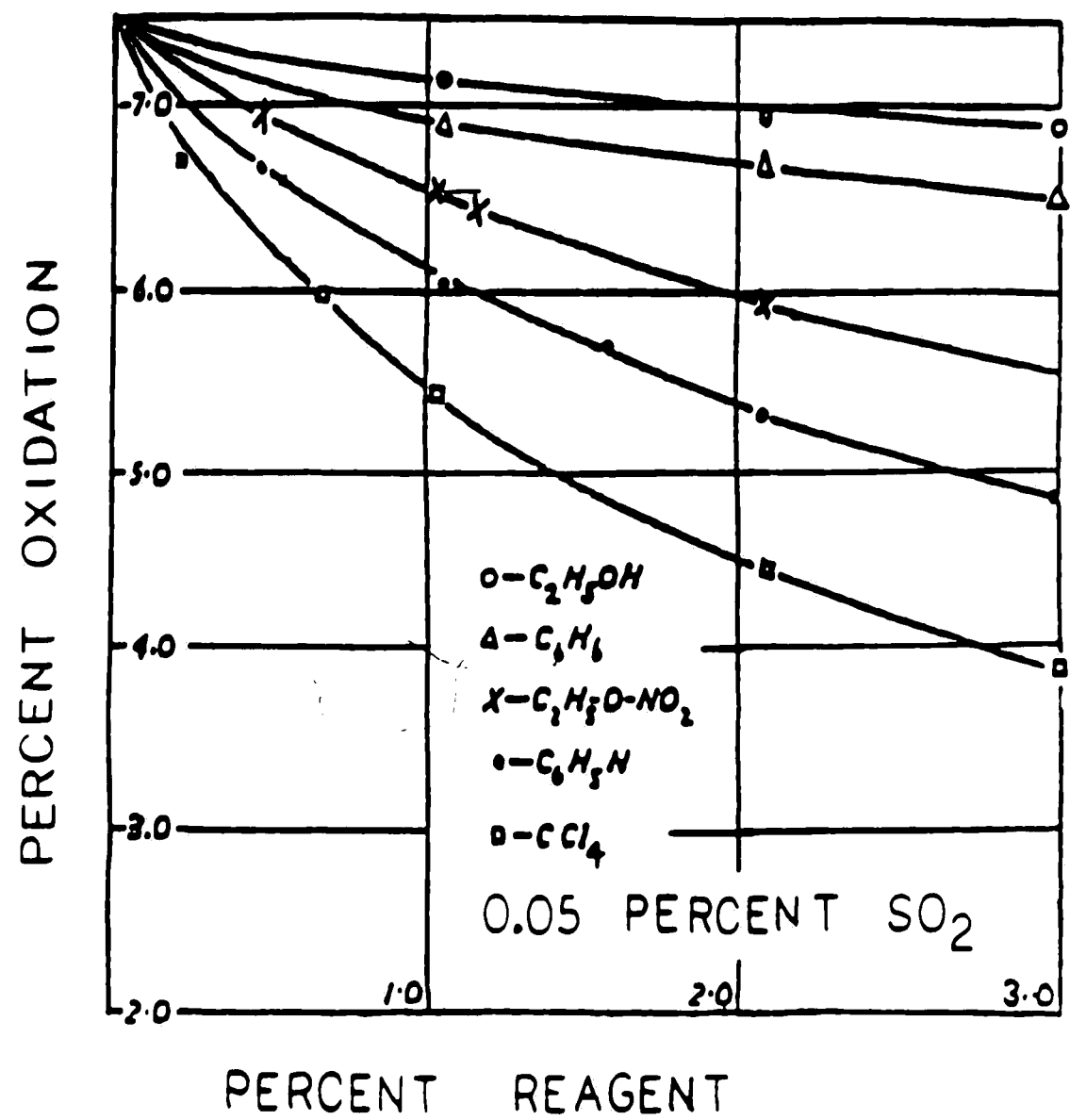


Figure 3. Effect of Reagent Concentration on Sulfur Trioxide Conversion in a Bunsen Flame

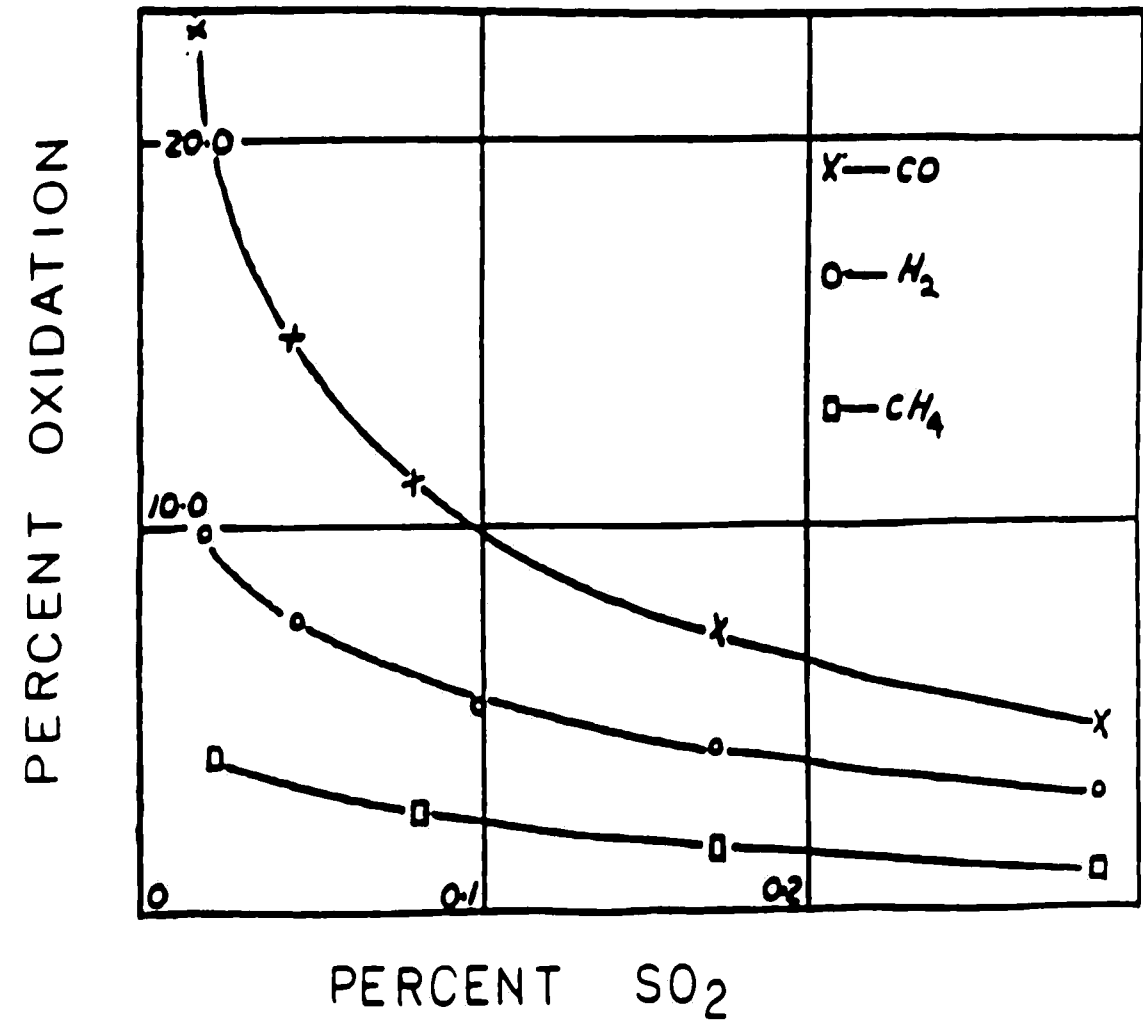
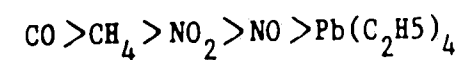


Figure 4. Sulfur Dioxide Oxidation in Various Bunsen Flames

available atomic oxygen.

Due to concern over possible interference of intermediate compounds formed when reagents were added directly to the fuel gas, Whittingham<sup>5</sup> redesigned the Bunsen-flame experiment to focus on the effects of flame inhibitors and catalysts on the product gases of coal-gas flames. Gas samples from the flame were removed through a sampling tube while sulfur dioxide, flame catalysts, and inhibitors were added to sidearms in the sampling tube. Oxidation to sulfur trioxide followed the order:

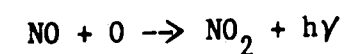


The lead-based oxygen scavenger produced the lowest conversions, with carbon monoxide generating the largest conversion. Also, conversion with nitric oxide was lower than that with methane, indicative of the oxygen-scavenging characteristics of nitric oxide. Because the order of oxidation followed the order of oxygen-atom availability, it was concluded that the reaction scheme involved atomic oxygen.

Gaydon<sup>6</sup> conducted discharge tube experiments with sulfur dioxide and oxygen mixtures in search for conclusive evidence of a luminous reaction between sulfur dioxide and atomic oxygen



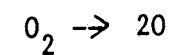
as occurs with nitric oxide



The mixture was passed through a discharge tube at low pressures while exposed to electric discharge, thereby generating atomic oxygen by dissociation of molecular oxygen. The mixture did not produce a glow, even with slight heating. However, sulfuric acid was found on the wall of the tube after the experiment. Apparently, sulfur trioxide was

generated by the non-luminous association of sulfur dioxide and atomic oxygen, suggesting absorption of the association energy by third bodies.

Fenimore and Jones<sup>7</sup> further elucidated characteristics of the processes involved in sulfur trioxide generation by measuring oxygen radical concentrations at different locations in a lean hydrogen flame. Atomic oxygen profiles were inferred by introducing isotopically-labeled water molecules into the fuel, and following the incorporation of isotopes in the flame products through use of mass-spectrographic techniques. Sulfur dioxide and sulfur trioxide profiles were obtained from analysis of sampled gases from flame traverses. The feasibility of various reaction schemes was determined by comparing species concentrations based on thermodynamic limits for a particular reaction to concentrations determined experimentally at 1600°K. Atomic oxygen levels exceeded those permitted by thermodynamics for thermal dissociation of molecular



oxygen, indicating the importance of alternative routes to atomic oxygen formation. The maximum observed ratio of sulfur trioxide to sulfur dioxide was 0.014.

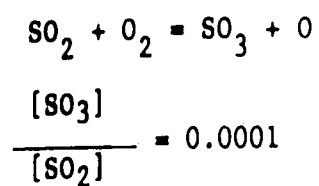
$$\frac{[SO_3]}{[SO_2]} = 0.014$$

For the reaction  $SO_2 + 1/2 O_2 = SO_3$  the calculated equilibrium ratio

$$\frac{[SO_3]}{[SO_2]} = 0.0027$$

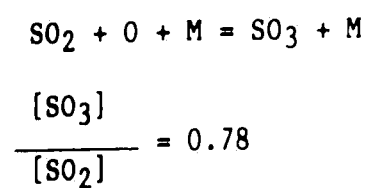
was lower than the observed conversion, indicating the presence of

another reaction path. The equilibrium ratio of sulfur trioxide to sulfur dioxide for the reaction



was less than the observed value, indicating another reaction pathway.

For the reaction



the calculated equilibrium conversion was greater than the observed value. Therefore, this reaction is a possible route to sulfur trioxide formation. Because the observed levels were lower than the limiting values, the reaction either proceeds slowly, never attaining the thermodynamic limit, or decomposition of sulfur trioxide occurs.

#### 2.4 The Decomposition of Sulfur Trioxide

The essence of the sulfur trioxide decomposition process was recognized by Merryman and Levy<sup>8</sup> by consideration of the interaction of flame pressure and sulfur trioxide distributions in the post-flame region. In their study of pre-mixed hydrogen sulfide and carbonyl sulfide flames, maximum concentrations, ultimate conversions, and decomposition extent depended on system pressure, as shown in Figure 5.

The ultimate amount of sulfur trioxide formed and the maximum conversion in a given flame system increased with pressure. The rate of formation of sulfur trioxide also increased with pressure. At lower pressures, the depletion of sulfur trioxide was more apparent. A reduction in sulfur trioxide formation rate is expected at lower pressures due to the reduced collision frequency between sulfur dioxide and oxygen.

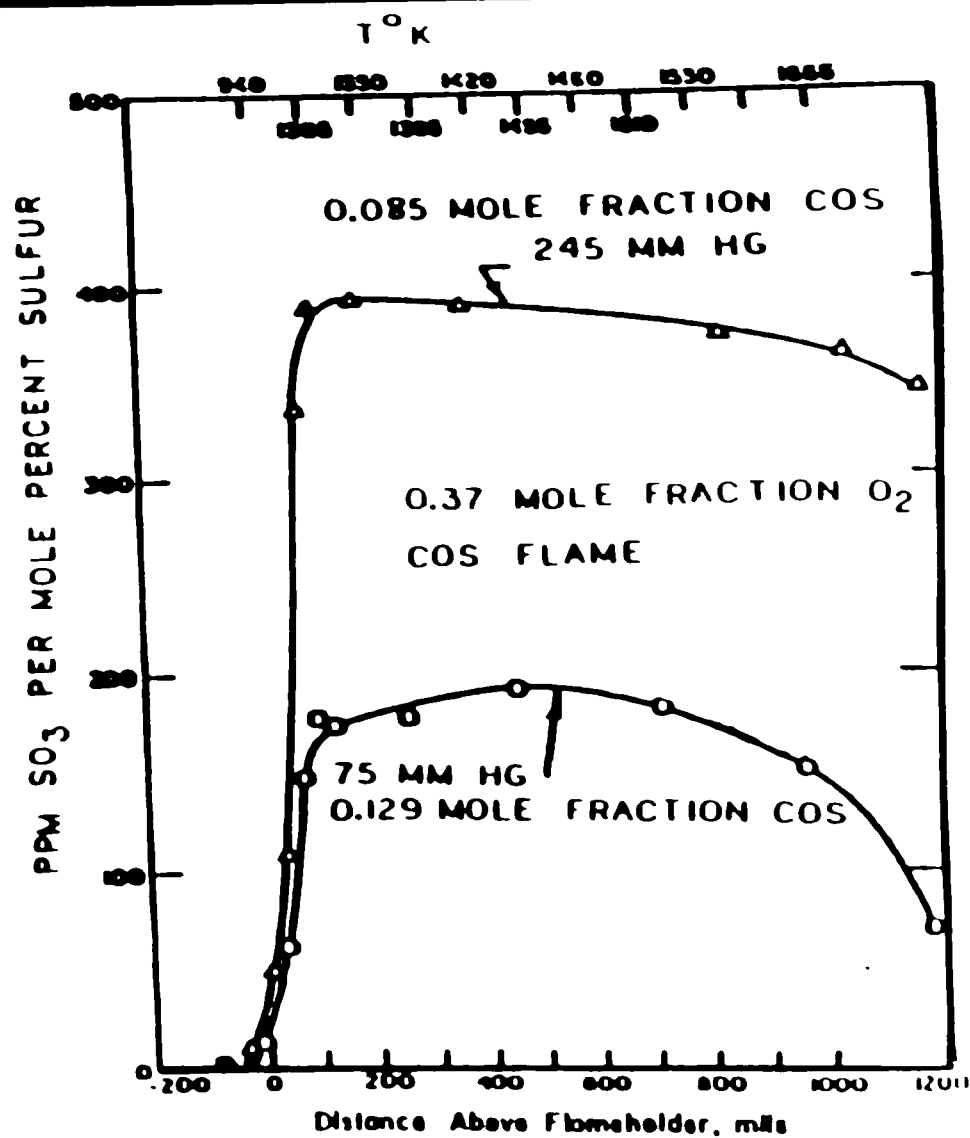
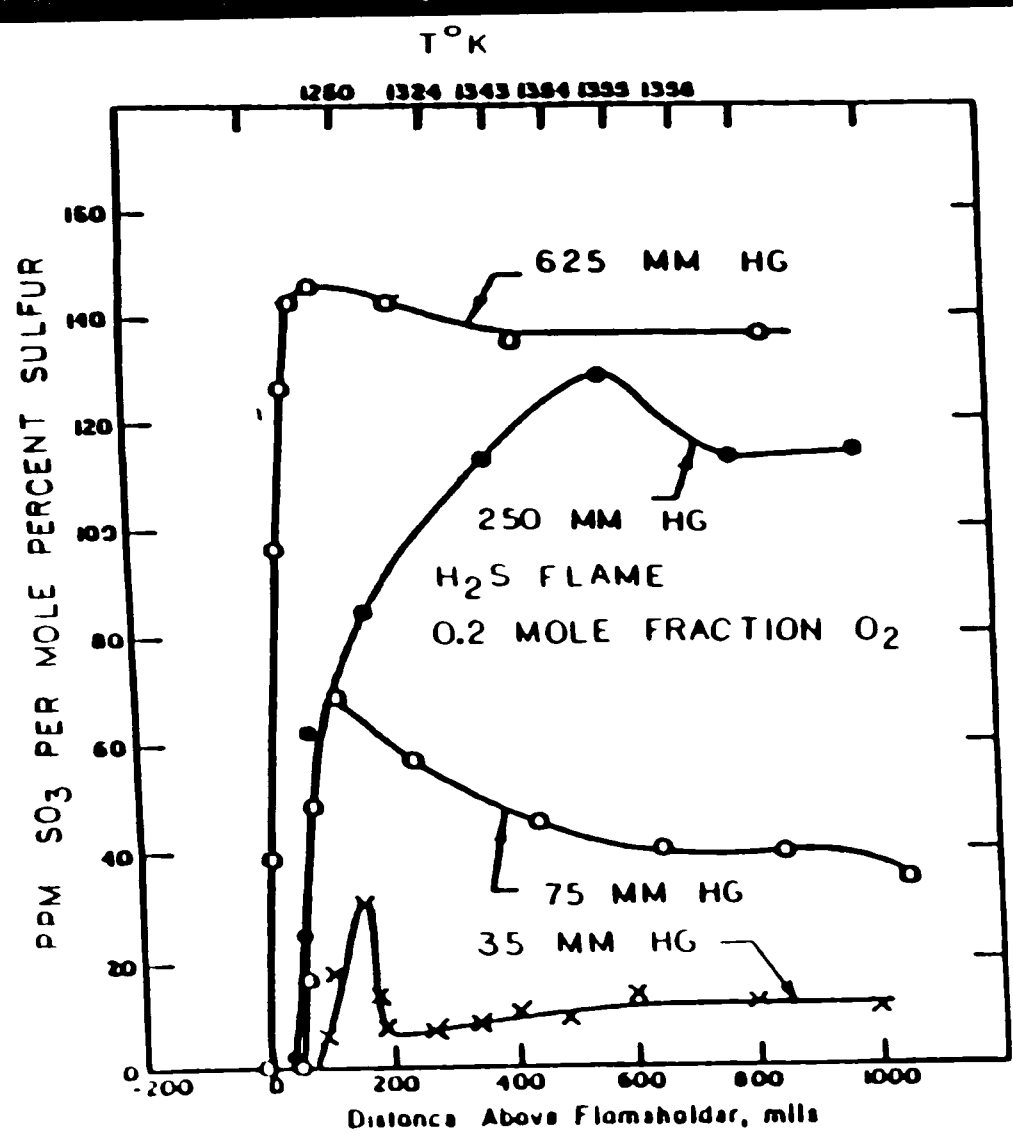
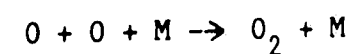
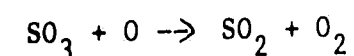


Figure 5. Pressure Effect on Sulfur Trioxide Profiles in Hydrogen Sulfide Flames and Carbonyl Sulfide Flames

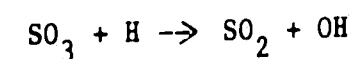
If the decomposition reaction involved only sulfur trioxide, decomposition rate would decrease with pressure. Therefore, another species with higher concentrations at low pressures must be involved, a characteristic of radicals like oxygen. The concentrations of radicals in the far post-flame region are higher at low pressure due to reduction in the recombination rate via:



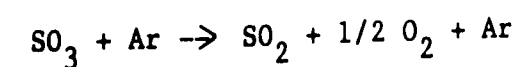
The decomposition reaction is therefore a temperature-dependent rate-limited reaction.



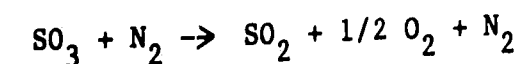
Lower conversions in the hydrogen sulfide flame compared to the COS flame suggest an additional mechanism involving hydrogen radicals



The reduced conversions might also be due to the lower temperatures. An alternative path for decomposition was demonstrated by Nettleton and Stirling.<sup>9</sup> Decomposition rates were measured by monitoring the emission record of a shock-heated mixture containing sulfur trioxide and argon at 1740°K. Direct decomposition to sulfur dioxide occurred in the absence of oxygen. The magnitude of the reaction-rate constant for



was eight times greater than the corresponding reaction involving nitrogen.



Therefore, the identity of the collision partner influences the decomposition rate.

The distribution of oxygen atoms in the flame directly influences



the relative effectiveness of the forward and reverse reactions which dictate sulfur trioxide conversion. Other species may also interact directly in the process. The concentrations of any radical in the flame and product gases are set by fast equilibrium reactions involving the components. Radical concentrations depend on the temperature, identity, and quantity of compounds present. Thus, conversion ultimately depends on the compounds available in a flame, the distribution of the compounds in the reaction zone, and the temperature distribution in which combustion takes place.

#### 2.5 The Effect of Excess Oxygen

Sulfur trioxide forms mainly in the post-flame region after the majority of hydrocarbon substituents have reacted. The effect of reducing excess air-levels to stoichiometric values is to minimize post-flame oxygen, reducing the conversion of sulfur to sulfur trioxide throughout the furnace. Hedley<sup>1</sup> observed this effect in studies with a pilot-scale furnace, as shown by his data in Figure 6. Stoichiometric conditions eliminated both intermediate and exit acid throughout the furnace. There was no decisive relationship between exit sulfur trioxide concentrations and oxygen levels. The principal effect of excess oxygen was observed in the intermediate regions of the furnace, where an increase in oxygen level resulted in a larger conversion to sulfur trioxide. Once the concentration reached a maximum in the intermediate region, the sulfur trioxide level decreased continuously throughout the remaining furnace region. The data suggests that further reductions in sulfur trioxide concentrations would have been realized if the furnace had been lengthened.

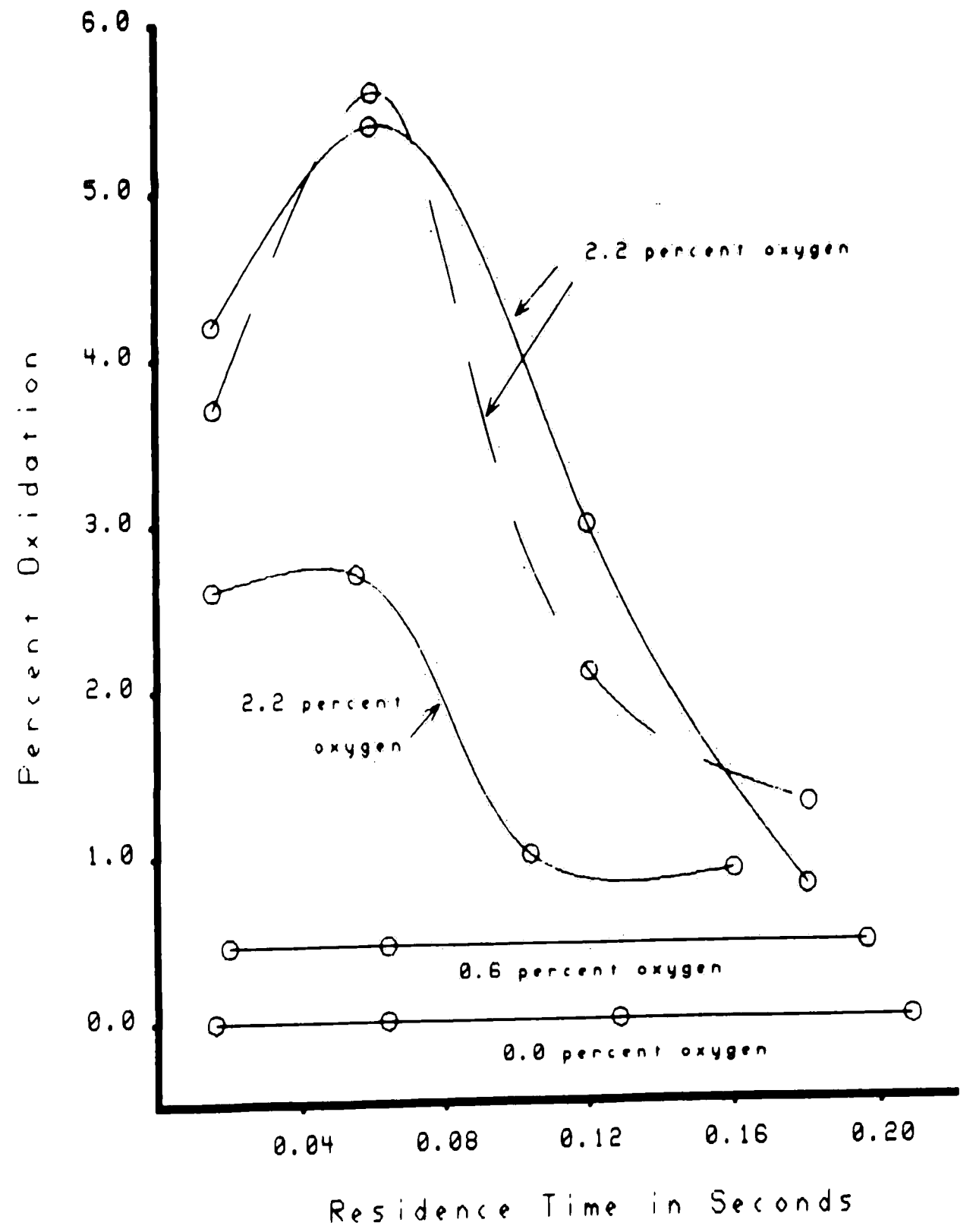


Figure 6. Sulfur Trioxide Profiles at Various Oxygen Levels in an Adiabatic Kerosene Furnace

Barrett, Hummell, and Reid<sup>10</sup> measured sulfur trioxide concentration profiles in a cooled-wall stainless steel combustor burning sulfur-doped natural gas. These results are shown in Figure 7. The sulfur trioxide concentration profile did not exhibit a maximum as in Hedley's measurements, but was uniform all the way to the exit of the combustion chamber. In addition, the sulfuric acid concentration in the gases exiting the furnace could be minimized by reducing the furnace oxygen level as shown in Figure 8, contrary to Hedley's results. The lack of evidence for sulfur trioxide decomposition in the Barrett et al. measurements is likely the result of the cooling of combustion gases by the combustor walls (shown in Figure 9) which reduces the rates of the sulfur trioxide decomposition reactions. Hedley observed the effect of the decomposition reactions because the combustion gases were not cooled by the furnace walls.

#### 2.6 Sulfur Trioxide Formation in a Utility-Boiler Flame

Sulfur trioxide can be present in the flue gases of a utility boiler as a result of the association of sulfur dioxide and atomic oxygen in the post-flame region of the furnace. Sulfur trioxide formed in the pre-flame region decomposes in the visible-flame region of the flame, and will not contribute to the flue-gas sulfur trioxide level. The amount of sulfur trioxide formed will depend on the relative rates of the post-flame formation and decomposition reactions. The rates of these reactions depend on the availability of the molecular and radical species participating in the reactions, the furnace-temperature distribution, and the mixing characteristics of the furnace.

Sulfur dioxide, hydrogen, and oxygen participate directly in the post-flame formation and decomposition reactions from which sulfur trioxide is generated. The amount of sulfur and hydrogen released by the

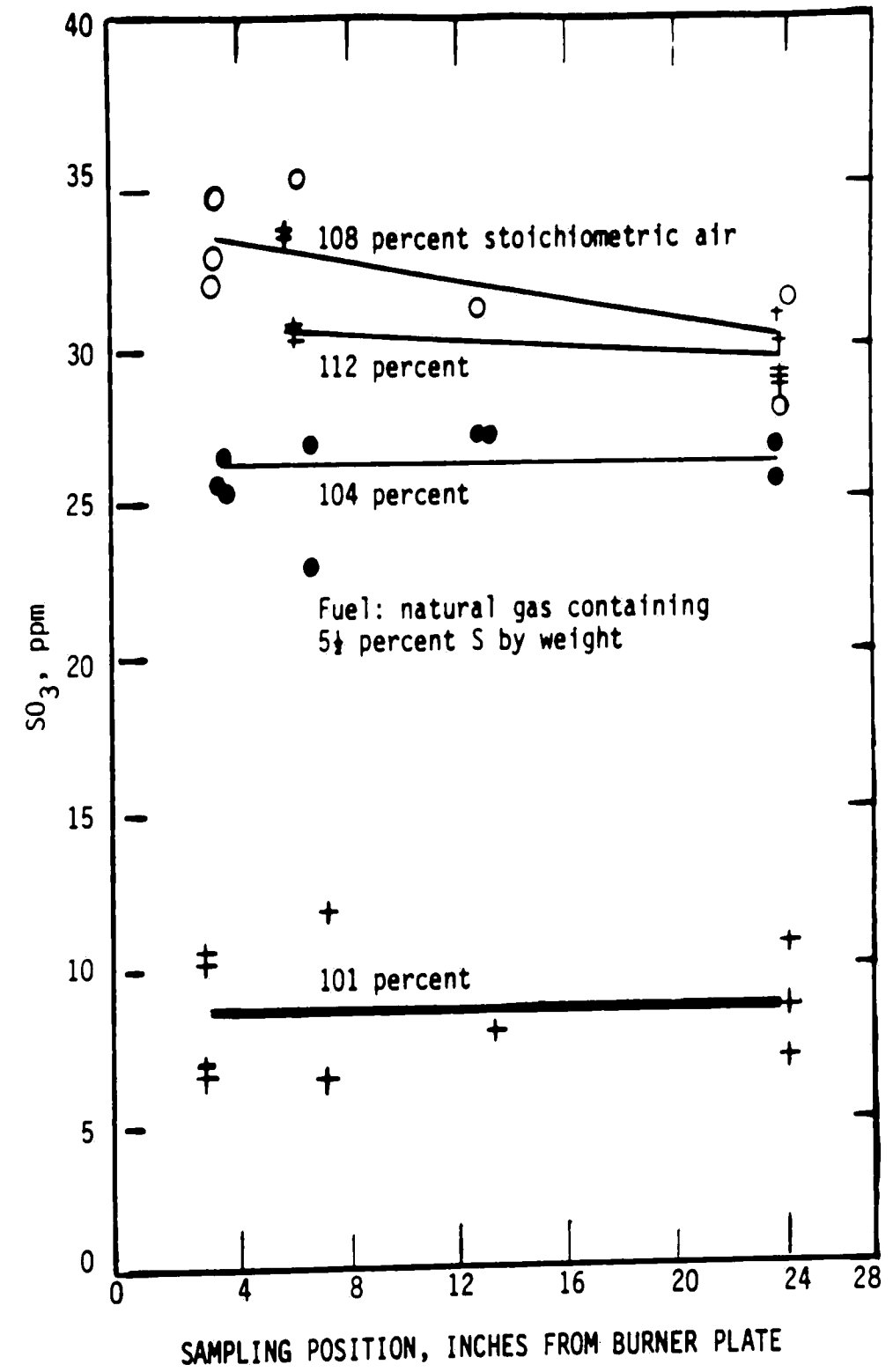


Figure 7. Sulfur Trioxide Profiles at Various Oxygen Levels in a Non-Catalytic Furnace with Wall Cooling

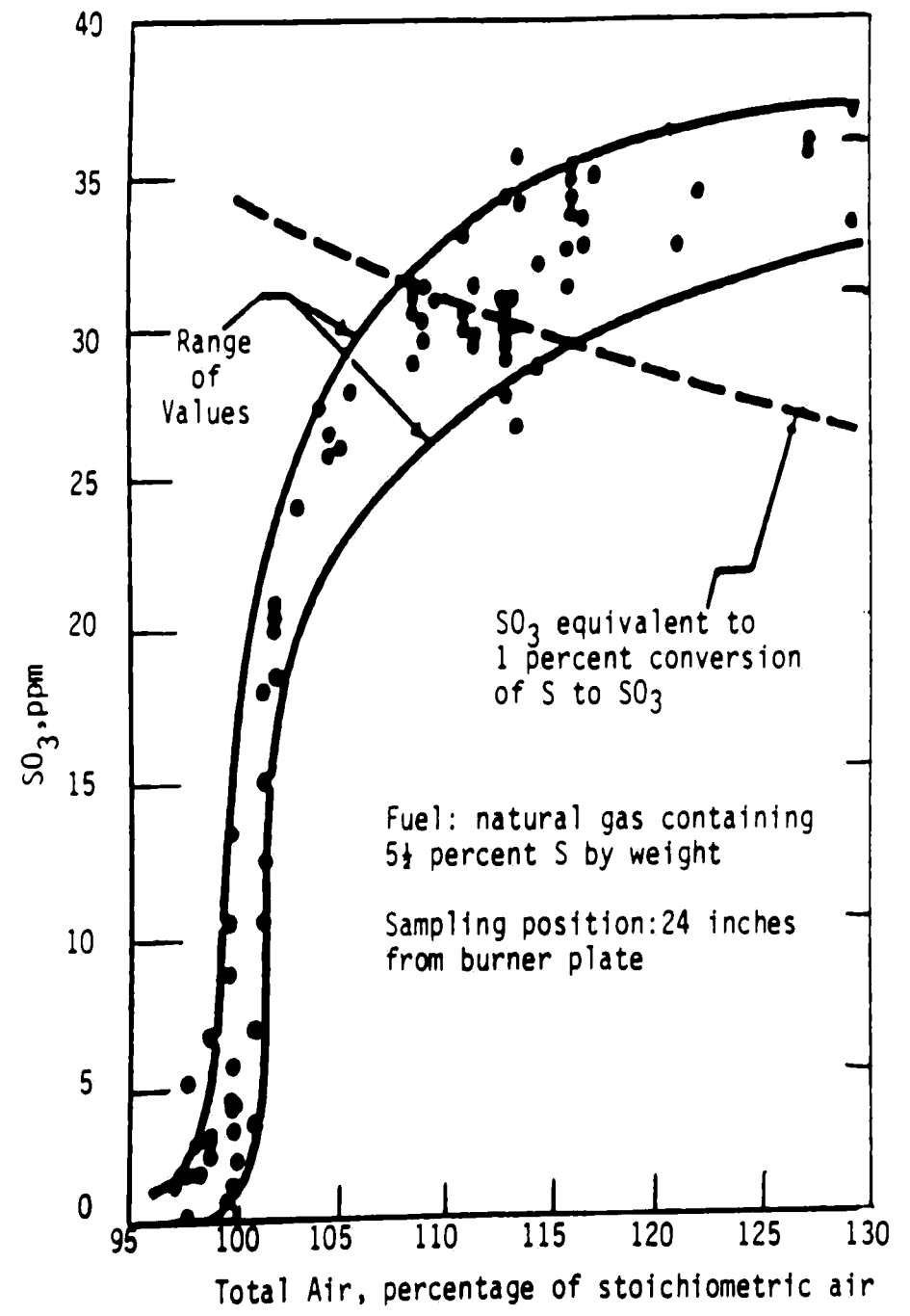


Figure 8. Sulfur Trioxide Concentration as a Function of Oxygen Level in the Non-Catalytic Furnace with Wall Cooling

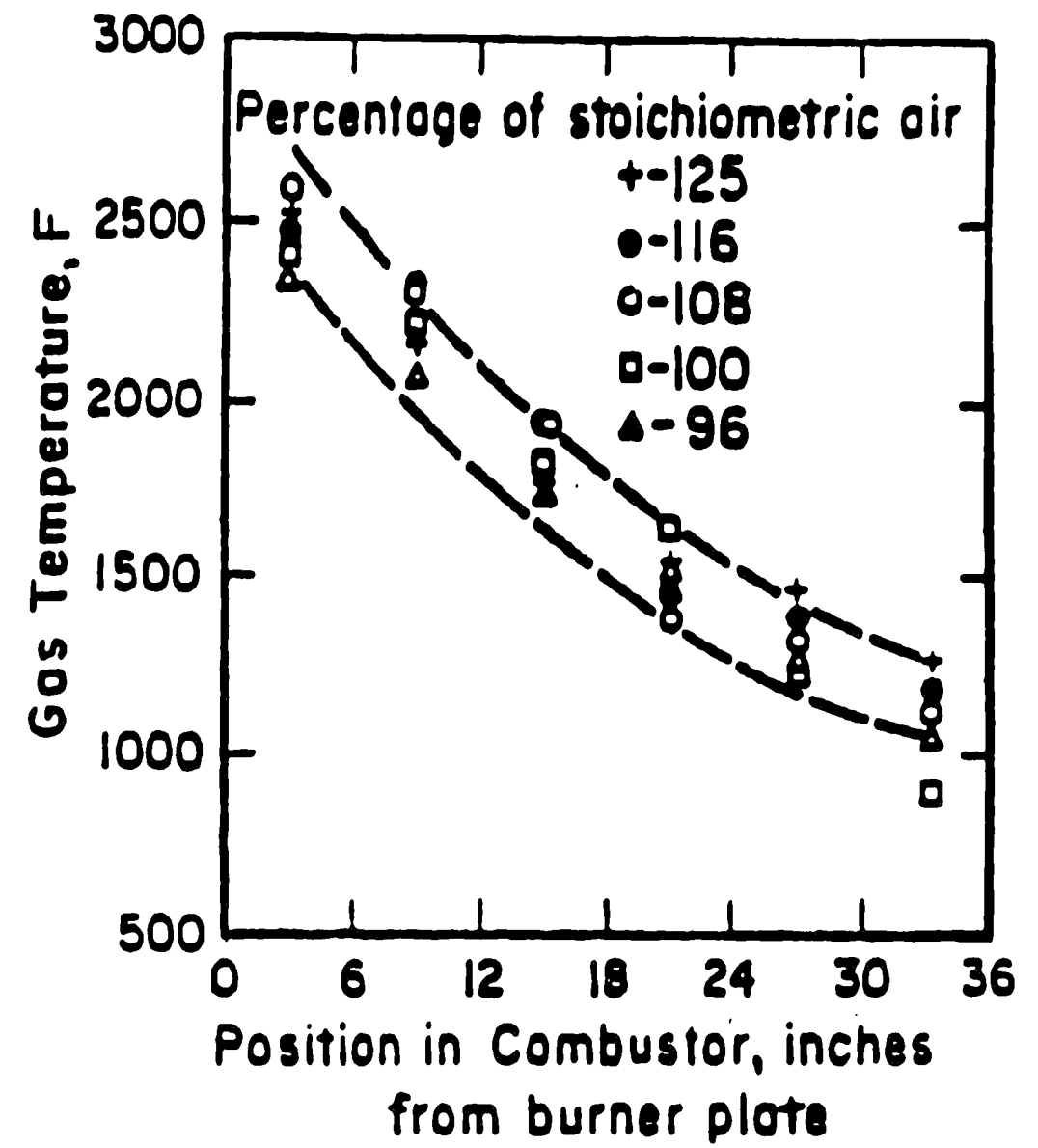


Figure 9. Temperature Distribution in the Non-Catalytic Furnace with Wall Cooling

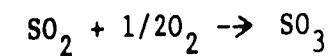
coal to the flame, and the amount of oxygen used to support the flame will therefore affect the amount of sulfur trioxide generated.

However, the sulfur and hydrogen content of the coal may not be related to the sulfur trioxide concentration in the flue gases, due to the presence of reactions which compete for these compounds.

The reactions which generate and destroy sulfur trioxide molecules in the post-flame region of the furnace proceed at rates which are temperature and concentration dependent. The furnace temperature distribution and the concentration distribution of the reactive compounds govern the amount of sulfur trioxide present in a flue gas resulting from the association of atomic oxygen and sulfur dioxide. Because furnace temperature distribution and mixing characteristics are cast in the boiler design, there is limited control of the sulfur trioxide reactions through operational modification of furnace temperature and mixing. The quantities of sulfur trioxide found in flue gases and the relative influence of excess oxygen and coal composition on flue-gas sulfur trioxide levels will vary from boiler design to boiler design.

### 3. CATALYTIC OXIDATION OF SULFUR DIOXIDE

Sulfur dioxide levels in a pulverized-coal flue gas are typically around 2000 ppm while excess oxygen levels range from one to five percent. The sulfur dioxide is subject to oxidation by molecular oxygen to form sulfur trioxide.



The equilibrium conversion is dependent on temperature and oxygen concentration as shown in Figure 10. At the high temperatures characteristic of the furnace (1100°C), conversion to sulfur trioxide by this reaction is negligible. Equilibrium conversion corresponding to temperatures below 400°C, characteristic of the colder sections of the heat recovery section, is nearly complete. These curves represent the upper limits for conversion to sulfur trioxide. In practice, less than one percent of the sulfur dioxide is converted to sulfur trioxide. The maximum limits set by thermodynamics are not attained due to the negligible rate of the reactions, even at high temperatures. The fraction of the total sulfur trioxide in the flue gas resulting from this reaction is small except when a catalyst is present to increase the rate of reaction. Iron present in the waterwall tubes and in the mineral deposits on the furnace wall (slag) can develop catalytic activity for this reaction.

An iron-containing material develops catalytic activity for sulfur dioxide oxidation by oxidizing to iron oxide. Conversion to this form involves a sequence of chemical and physical changes in the iron-containing surface. Tolly's<sup>12</sup> data shown in Figure 11 demonstrate the time dependence of catalytic activity development. When a clean steel tube held at 600°C was first exposed to a flow of



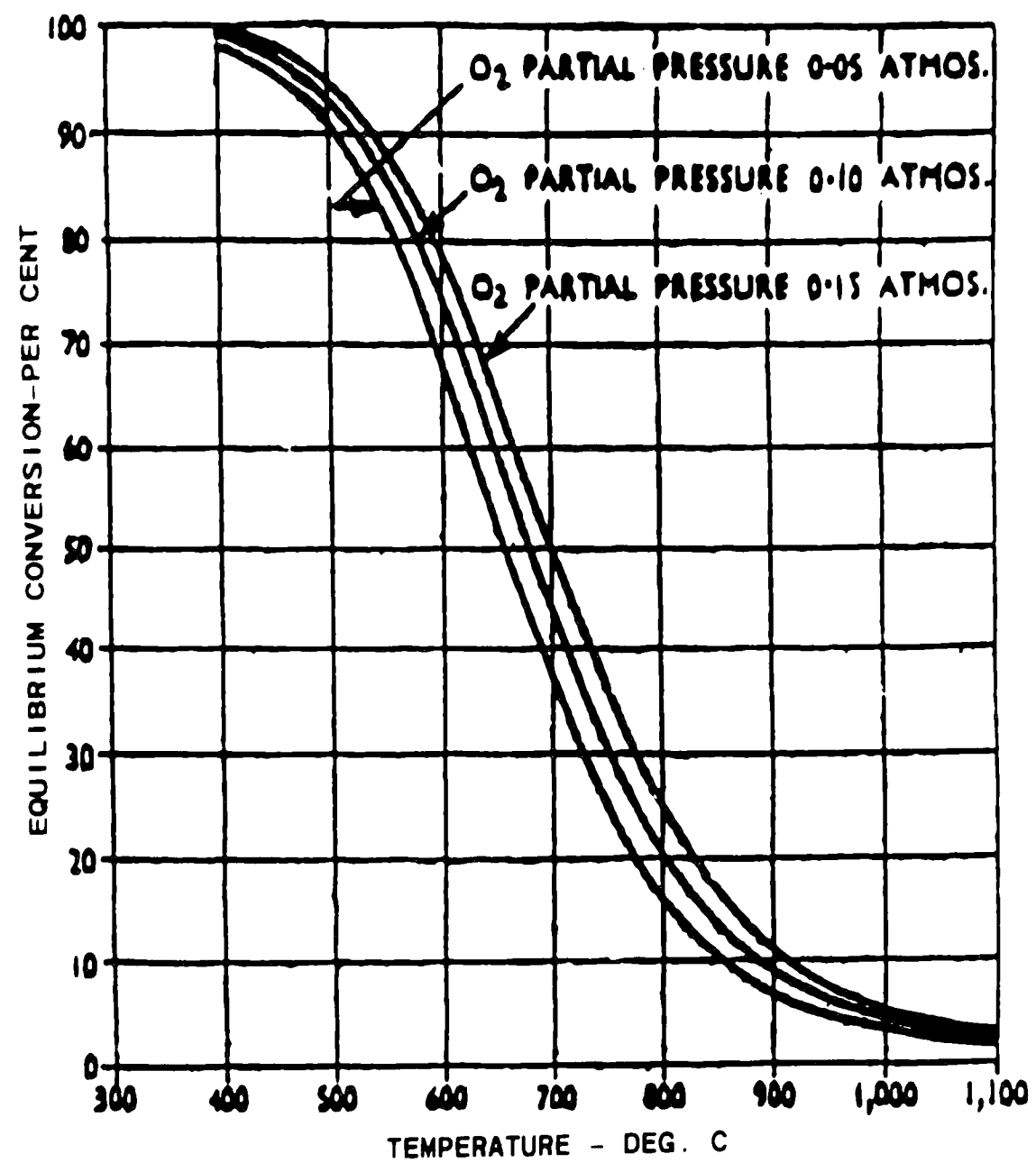


Figure 10. Equilibrium Conversion as a Function of Temperature for the Reaction<sup>11</sup>  $\text{SO}_2 + 1/2 \text{O}_2 \rightarrow \text{SO}_3$

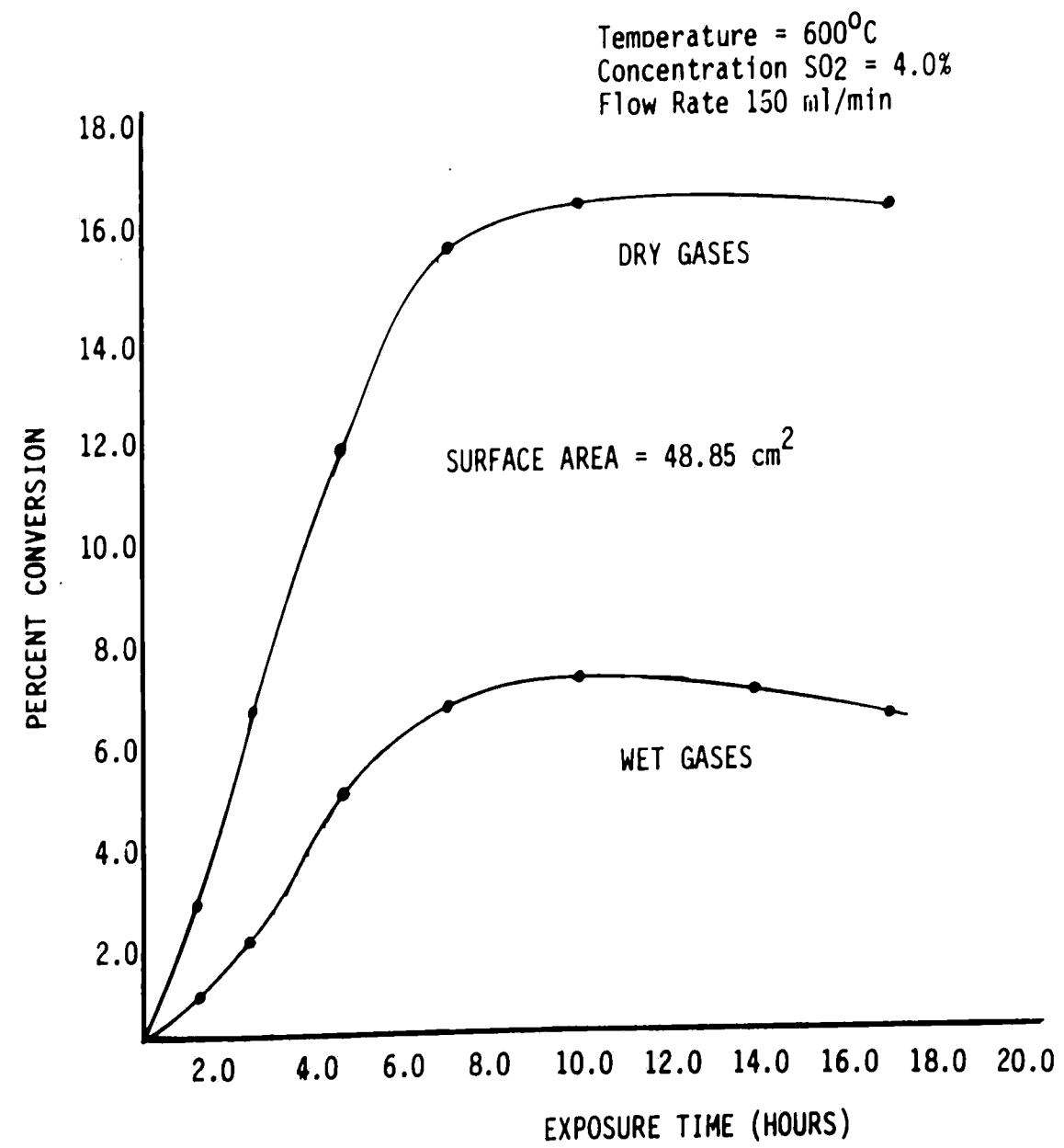
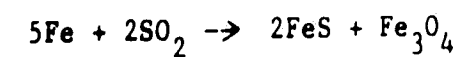


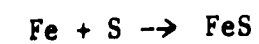
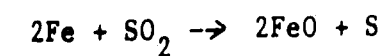
Figure 11. Catalytic Activity Development Time Dependence for a Steel Tube

sulfur dioxide and oxygen, little conversion to sulfur trioxide occurred. The conversion to sulfur trioxide increased rapidly with continued exposure, leveling off after ten hours. Tolly established the chemical and physical changes from analysis of the scale on the tube surface at different stages of the catalytic development.

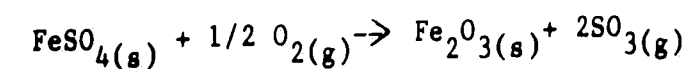
In the early stages of exposure, direct reaction between iron and sulfur dioxide gives both ferrous sulfide and ferrous oxide.



Above 570°C, additional consecutive reactions are operative.



These reactions cause an increase in surface area due to the formation of a porous scale. Reactions between sulfur dioxide and iron produce sulfate which partially decomposes into iron oxide and sulfur trioxide. This reaction



is the principle source of iron oxide. The expanding surface area generated by scale-formation reactions increases contact between the iron oxide and sulfur dioxide resulting in enhanced sulfur trioxide formation. Small amounts of iron oxide and ferrous oxide are formed by direct oxidation of iron by oxygen. Once the scale has developed to the thickness such that the diffusion rate of iron to the gas interface is small, thermodynamics sets the distributions between iron sulfate, iron oxide, gaseous oxygen, and sulfur trioxide.

The ability of an iron surface to develop catalytic activity is temperature dependent, as shown by Tolly and others.<sup>12,13,14</sup> The ability of a mild steel surface below 400°C to develop catalytic

capacity and to promote sulfur dioxide oxidation is negligible, as shown by Tolly's data presented in Figure 12. Catalytic activity develops at higher temperatures allowing thermodynamic conversions to be realized. Because the maximum conversion set by thermodynamics decreases with temperature, a maximum in conversion occurs at 650°C. Above this temperature, conversion is reduced. At the lower temperatures, less iron oxide is formed from iron sulfate decomposition, reducing the catalytic capacity of the surface. The ability of iron oxide to catalyze sulfur dioxide oxidation is reduced at low temperatures, as shown by Barrett's<sup>10</sup> data in Figure 13. The presence of water vapor in the gases also reduces the catalytic effectiveness of the surface, as shown by Tolly's data in Figure 11. The inhibiting effect of water is attributed to the direct oxidation of iron to form  $Fe_3O_4$ , which is catalytically inert.

In Tolly's flow experiments, the conversion of sulfur dioxide to sulfur trioxide was inversely proportional to the gas velocity over the surface, as shown by his data plotted in Figure 14. Gas velocity is related to the extent of sulfur dioxide oxidation because catalytic oxidation is a rate process which depends on the contact time between the gas and the catalytic surface.

The amount of sulfur trioxide in a utility-boiler flue gas resulting from the catalytic oxidation of sulfur dioxide is expected to increase as boiler load is reduced, because contact time between catalytically active surfaces and flue gas increases as load is reduced. Due to the relationship between the rate of catalytic oxidation of sulfur dioxide, and the relationship between the equilibrium conversion for the homogeneous (catalytic) oxidation of

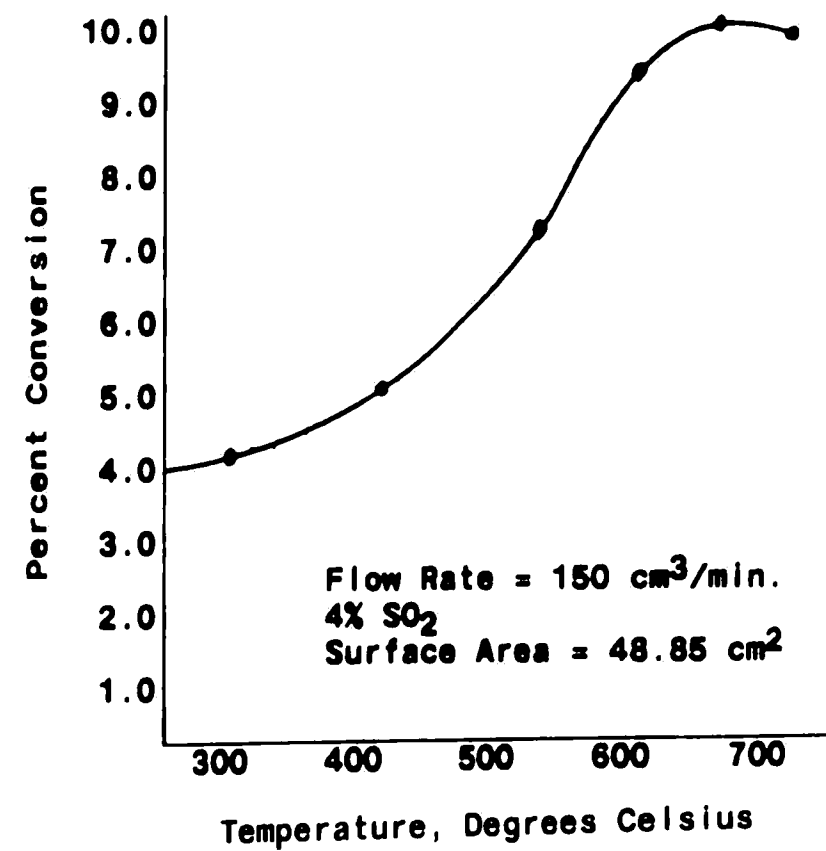


Figure 12. Catalytic Activity  
Temperature Dependence  
for a Steel Tube

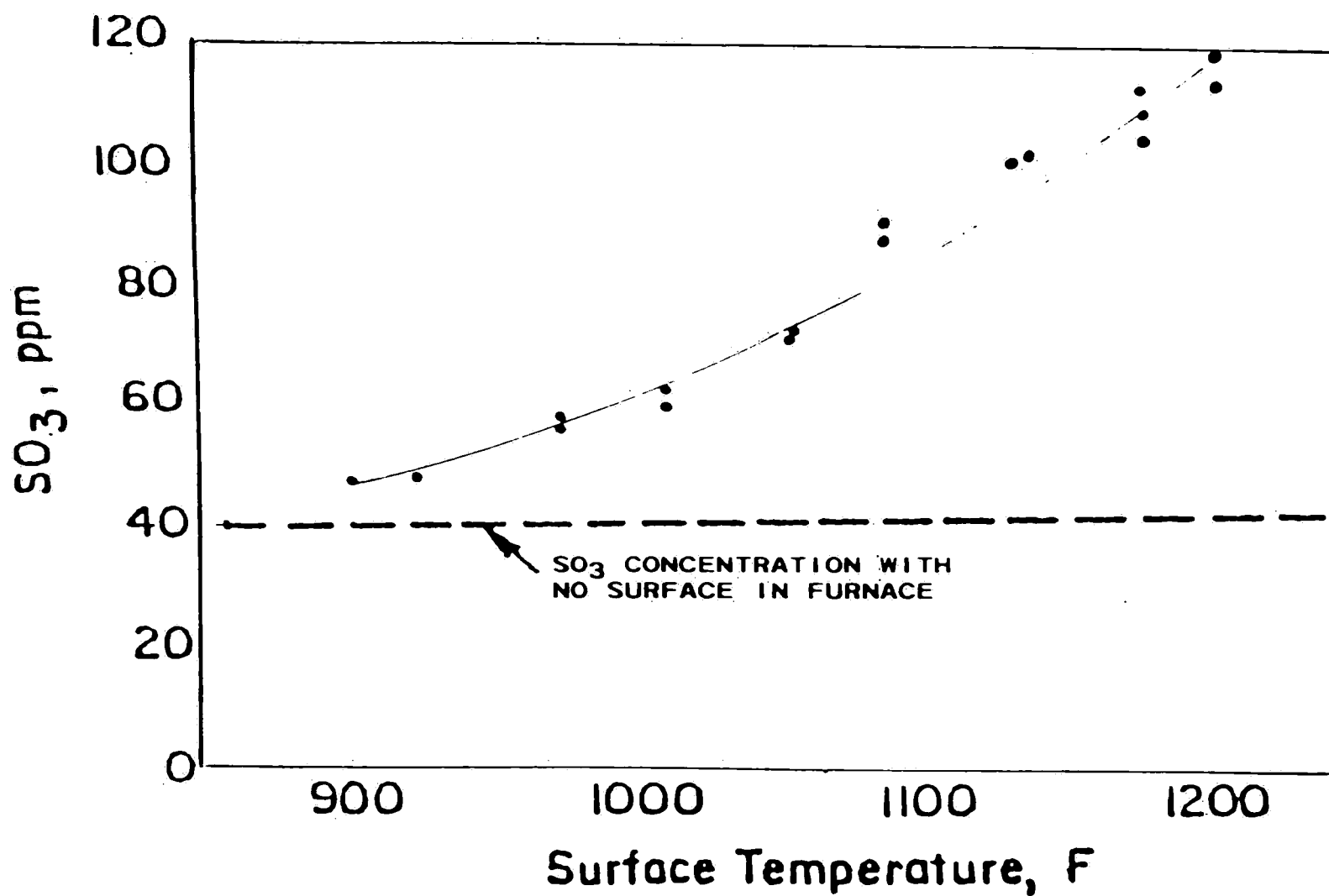


Figure 13. Catalytic Activity Temperature Dependence for an Iron Oxide Coated Surface

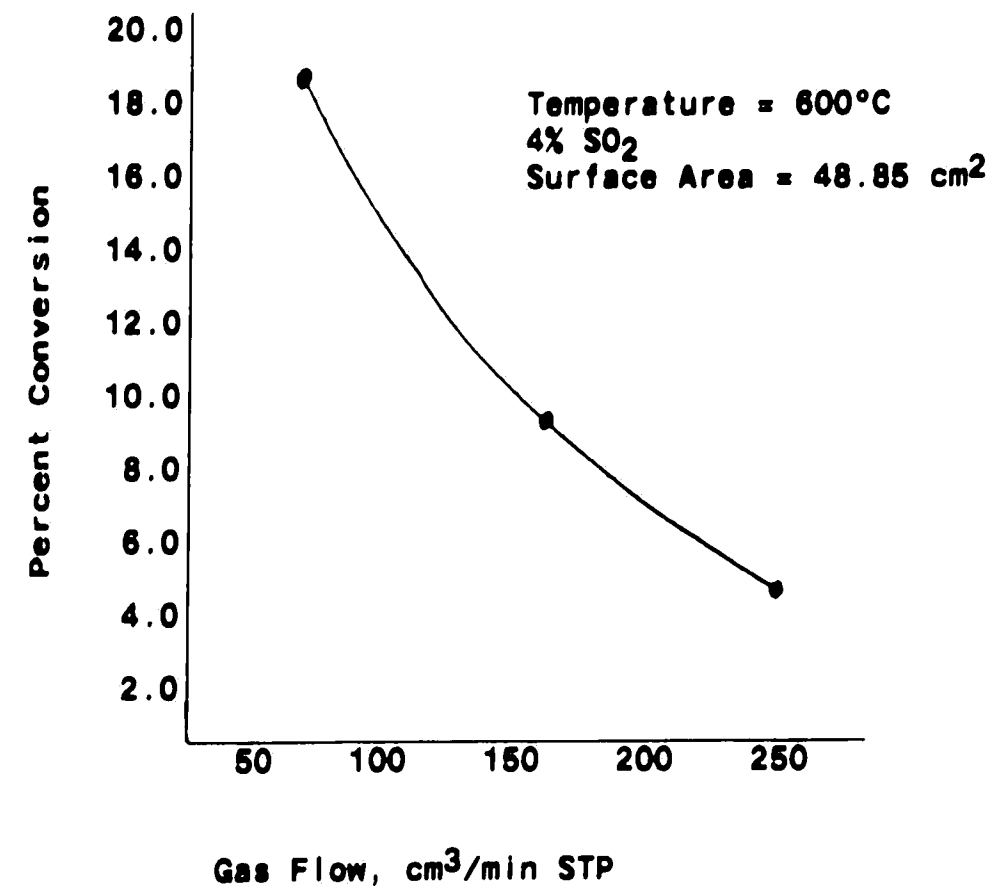


Figure 14. The Effect of Gas Flowrate on the Conversion of Sulfur Dioxide to Sulfur Trioxide by Catalytic Oxidation

sulfur dioxide and oxygen concentration, furnace oxygen level should also influence the amount of sulfur trioxide generated from the catalytic oxidation of sulfur dioxide. The amount of sulfur dioxide present in a flue gas will also affect the concentration of sulfur trioxide resulting from catalytic oxidation. The relative influence of unit load, flue-gas sulfur dioxide concentration, and furnace-oxygen level on sulfur trioxide concentration will depend on the degree of catalytic activity developed by the slag and water-wall tubes in a boiler. Because temperature and oxygen levels set the amount of iron oxide formed on such surfaces, the catalytic activity of surfaces in a boiler will depend on the operational history of the furnace.



#### 4. PULVERIZED-COAL COMBUSTION CHARACTERISTICS

The coal particles used for pulverized-coal firing are small, ranging in size up to 300 microns in diameter. As these particles enter the furnace through the burners, they are exposed to an oxygen-containing environment while being heated at a rate ranging between 1000 and 10,000°C per second. Figure 15 depicts the sequence of physical changes experienced by a coal particle during the combustion process. During the initial devolatilization (pyrolysis) stage, gaseous decomposition products are expelled from the surface with the concurrent formation of a liquid melt (known as tar) on the particle surface. The second devolatilization stage is characterized by the decomposition of the melt into additional gaseous products. Because volatiles are expelled at a rapid rate during the devolatilization stages, little oxygen reaches the particle surface and oxidation occurs in the gaseous zone surrounding the particle. Surface oxidation of the underlying char commences once devolatilization is essentially complete. Interstitial void areas are formed in the char during the heating associated with surface oxidation. Particle oxidation commences once the surfaces exposed during void formation support oxidation. High melting-point minerals present in the form of aggregates in the parent coal particle combine with nearby combustible material during the particle oxidation stages. The resulting mineral composites are found in the flue gases as ash particles because they are resistant to oxidation in the furnace due to their chemical composition and structure.

##### 4.1 Conversion of Sulfur Compounds

In general, about one half of the sulfur found in a coal resides in

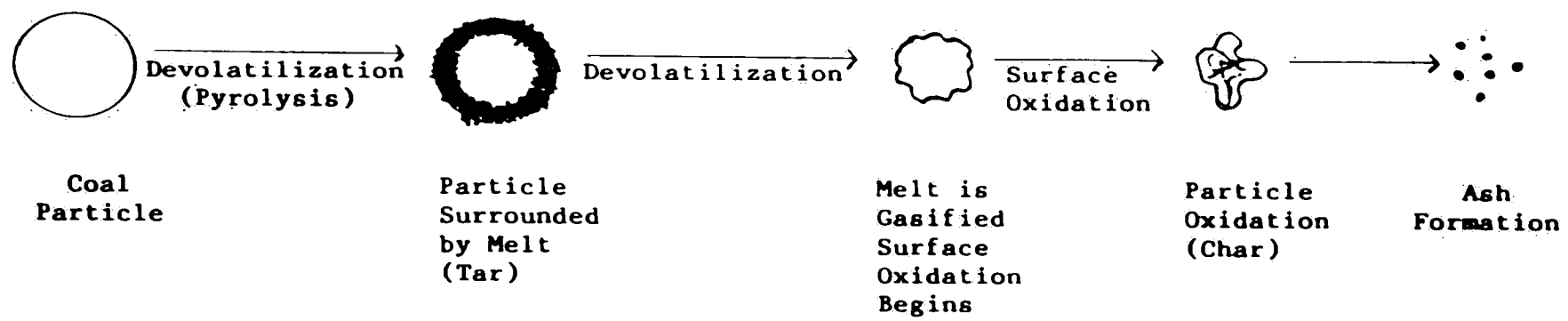
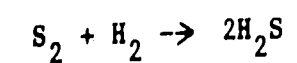
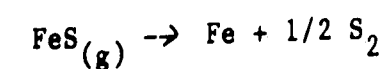
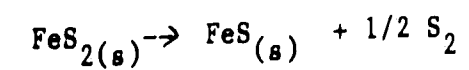


Figure 15. Sequence of Physical Changes During Particle Combustion

organic molecules, while the remaining portion is bound as inorganic pyrites and sulfates. Forms of organic sulfur are classified according to their relative resistance to thermal decomposition (Table I).<sup>17</sup> The temperature dependence of the evolution of hydrogen sulfide from a coal as measured by Yergey<sup>18</sup> using mass-spectroscopic techniques is presented in Figure 16.

Mercaptans, sulfides, and disulfides comprise the loosely-bound sulfur group known as Organic I. During the devolatilization stages of combustion, Organic I sulfur evolves directly as hydrogen sulfide. Organic II and Organic III sulfur is contained in heterocyclic rings, rendering it more resistant to thermal decomposition than Organic I. Sulfur contained in heterocyclic rings is also released into the gas as hydrogen sulfide during devolatilization.

Pyritic sulfur is sulfur bound to iron (an inorganic) which is more resistant to thermal decomposition than the organic forms. Pyritic sulfur decomposes by the successive reactions:



A fraction of the pyritic sulfur is incorporated into the tar and into the char as Organic P.

Organic P is organic sulfur which is formed during devolatilization as a result of reactions between reactive organic molecules and sulfur released during pyrite decomposition. Organic P is highly resistant to thermal decomposition, evolving with the tar as hydrogen sulfide during devolatilization or released to the gas during


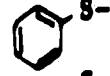
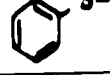

Group	Source	Structure
Organic I	Mercaptans	
	Sulfides	
	Disulfides	
Organic II Organic III	Thiophene and other Heterocyclic Rings	
Pyritic Sulfur	Pyrite	S-Fe-S
Organic P	Reactions between Pyritic Sulfur and Organic Molecules	Organic Sulfur

Table 1. Coal Sulfur Classification

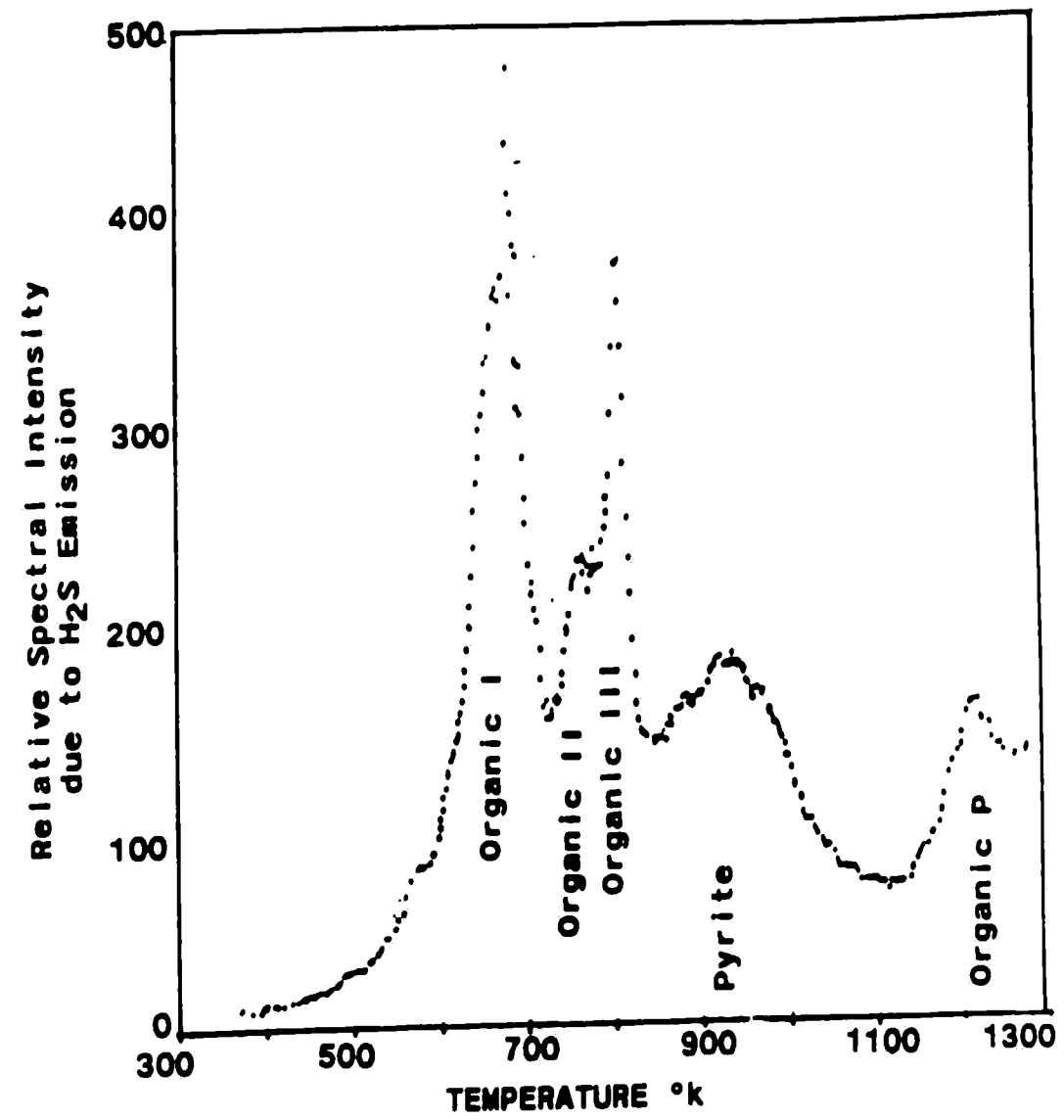


Figure 16. Temperature Dependence of H<sub>2</sub>S Emission from Coal (Reported in Spectral-Intensity Units)

char oxidation.

The primary form of sulfur released to the flame processes during devolatilization is hydrogen sulfide. The sulfur released during these stages combines with hydrogen due to the highly-reactive nature of hydrogen at high temperatures and because hydrogen is present in large excess. Once char combustion begins, the hydrogen content of the coal has been depleted, and the particle surface becomes oxidizing. Oxygen can then compete with available hydrogen for released sulfur.

A significant portion of the sulfur entering the furnace through the burners never reaches the flue gases. Gronhoud, Tufts, and Selle<sup>19</sup> measured the sulfur dioxide concentration (the primary form of gas-phase sulfur) in stack emissions from pulverized-coal-fired units for a variety of western-U.S. lignite coals and related the measurements to coal composition. The results of this study are presented in Figure 17. The sulfur content in the flue gases varied over a wide range and could not be correlated to the sulfur content of the parent coal. The sulfur concentration in emissions from units burning coal containing large amounts of  $\text{Na}_2\text{O}$  and  $\text{CaO}$  were lower than normal, while the presence of  $\text{SiO}_2$  and  $\text{Al}_2\text{O}_3$  in the parent coal tended to enhance the sulfur content in emissions. Analysis of the ash material associated with the sulfur-emission measurements showed that the sulfur which did not enter the flue gases was being retained as an integral part of the ash. The sulfur in the ash was complexed with calcium and sodium in the form of decomposition-resistant alkali sulfates, a reaction which apparently occurs during the coal-particle combustion process. Silicon and aluminum oxides were also complexed with the calcium and sodium in the coal. Sulfur emissions were greater when the coal possessed silicon

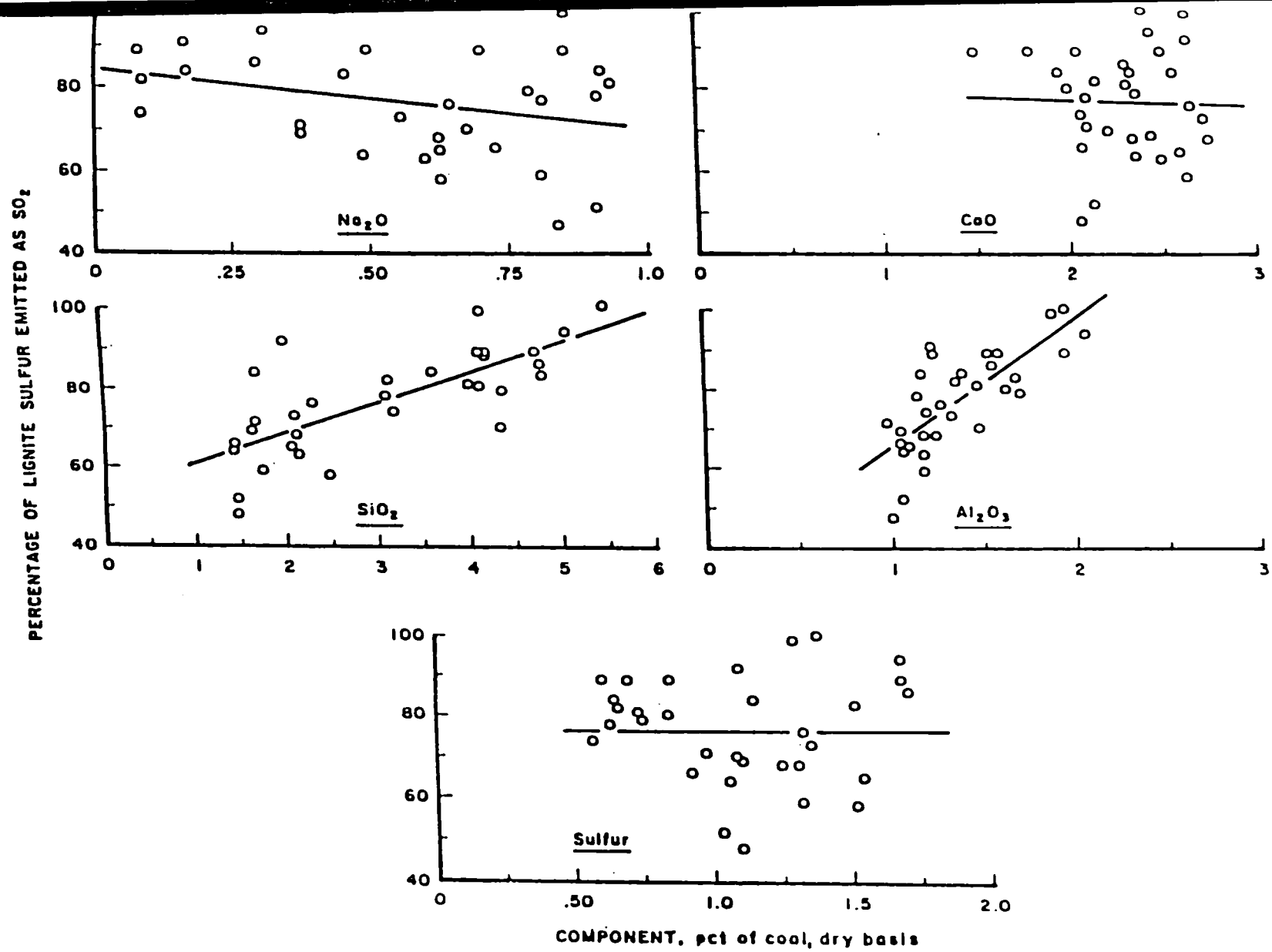


Figure 17. Smoke Stack Sulfur Dioxide Emissions Versus Parent Coal Mineral Composition

and aluminum oxides, because these compounds compete with sulfur for available calcium and sodium, thereby reducing the sulfur-retention effectiveness of the ash.

The composition of the parent coal will inevitably influence the amount of sulfur trioxide in a flue gas. Because sulfur trioxide can decompose to form sulfur dioxide and oxygen through collisions with hydrogen radicals in the post-flame region, the hydrogen content of the coal is expected to affect the amount of sulfur trioxide found in a flue gas. In addition, the amount of moisture in a flue gas depends on the hydrogen content of the coal, and flue-gas moisture reduces the ability of iron oxide to catalyze sulfur dioxide oxidation. The amount of sodium, calcium, silicon, and aluminum in the coal will also influence the amount of sulfur trioxide generated, because the concentration of these materials dictates the amount of sulfur released to the flame reactions and the quantity of sulfur dioxide available for catalytic oxidation.

#### 4.2 Furnace Temperature Distribution

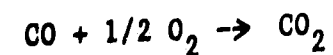
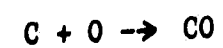
The amount of sulfur trioxide that forms as a result of flame reactions depends on the relative success of the reactions from which it formed and decomposed. These reactions are rate-limited reactions, possessing unique species-concentration and temperature dependencies. Because the conversion of sulfur to sulfur trioxide in a boiler flame depends on these reactions, operational parameters which influence species release rate and furnace temperature distribution are of interest.

Furnace temperature distribution is cast in the design used to construct the boiler. Burner location and design establishes the regions of energy release, while water-wall tube positioning and gas-flow



patterns determine where energy is transferred to the steam. The amount of heat removed at any location in a furnace is a function of the temperature difference between the combustion gases and the steam at that position, along with the corresponding resistances to thermal transport. The net resistance to thermal transport (excluding radiation) is the sum of convective and conductive contributions. Convective resistance is a function of combustion-gas flow rate and boiler feed-water flow, both of which are set by the boiler design and system load. Conductive resistance depends on the thickness of the solid material between the combustion gas and steam, and the associated thermal conductivity of the material. This solid material includes water-wall tube metal and deposited mineral material from the coal (slag). Because the deposition of mineral material is a continuous process, slag is periodically removed during operation by directing compressed air or high-pressure steam at the deposits (soot blowing). Slag thickness often exceeds water-wall tube thickness by several orders of magnitude in the course of normal operation. An extensive slag deposit may constitute the major resistance to thermal transport.<sup>20</sup> Because the slag distribution in a furnace affects the heat-removal rate, the slagging condition will affect the temperature distribution in a furnace.

During coal devolatilization, a capsule of reactant volatile material composed mostly of carbon and hydrogen surrounds the particle. Oxygen diffuses inward and participates in a gas-phase reaction sequence to form carbon dioxide.



Estimates of the time required to burn the volatiles as a function of coal particle size are given by Field<sup>21</sup> and are shown in Figure 18. The results of the calculation shown are for a partial pressure of oxygen = 0.0905 atmospheres, an ambient temperature of 1000°C, a mean molecular weight of volatiles of 100, and a volatile yield of fifty percent. Volatile yield and volatile mean molecular weight are functions of the heating rate and the specific coal used. The simulation shows that volatile burning time is reduced as coal particle size decreases. In addition, the model predicts that volatile burning time decreases as the oxygen concentration increases.

The influence of particle size on char-combustion rate was demonstrated in the laboratory by Field.<sup>22</sup> A flow of devolatilized coal particles (char) were introduced into a heated reactor tube. The residence time of the particles in the reactor was fixed by the tube length and the feed flowrate. The ratio of the mass of the feed stream to the amount of oxygen introduced was held constant, while the char size was varied. The mass of the char exiting the reactor was determined after rapid quenching of the reaction products. One set of Field's data is plotted in Figure 19. The fractional weight loss was greater for small particles than for large particles. Weight loss was greater for high-oxygen runs than it was for low-oxygen runs for the same size particles.

The trends exhibited during devolatilization and particle combustion are identical. Volatile release rate and surface combustion rates are greater for small particles than for large particles. In addition, the volatiles burn more rapidly in an atmosphere containing large amounts of oxygen than in an oxygen-deprived atmosphere.

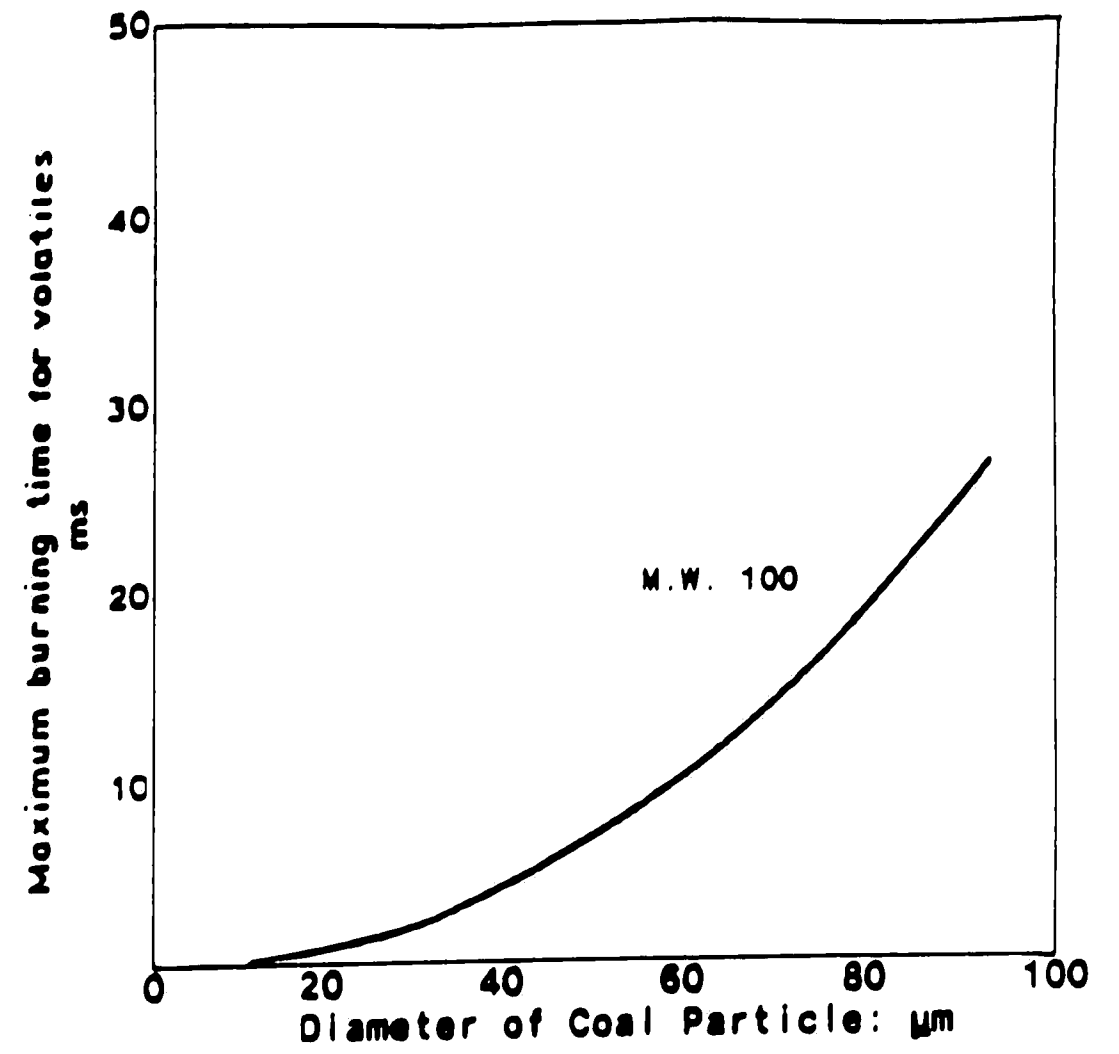


Figure 18. Simulated Volatile Burning Time as a Function of Coal Particle Size

1620 K  
27 MILLISECOND EXPOSURE

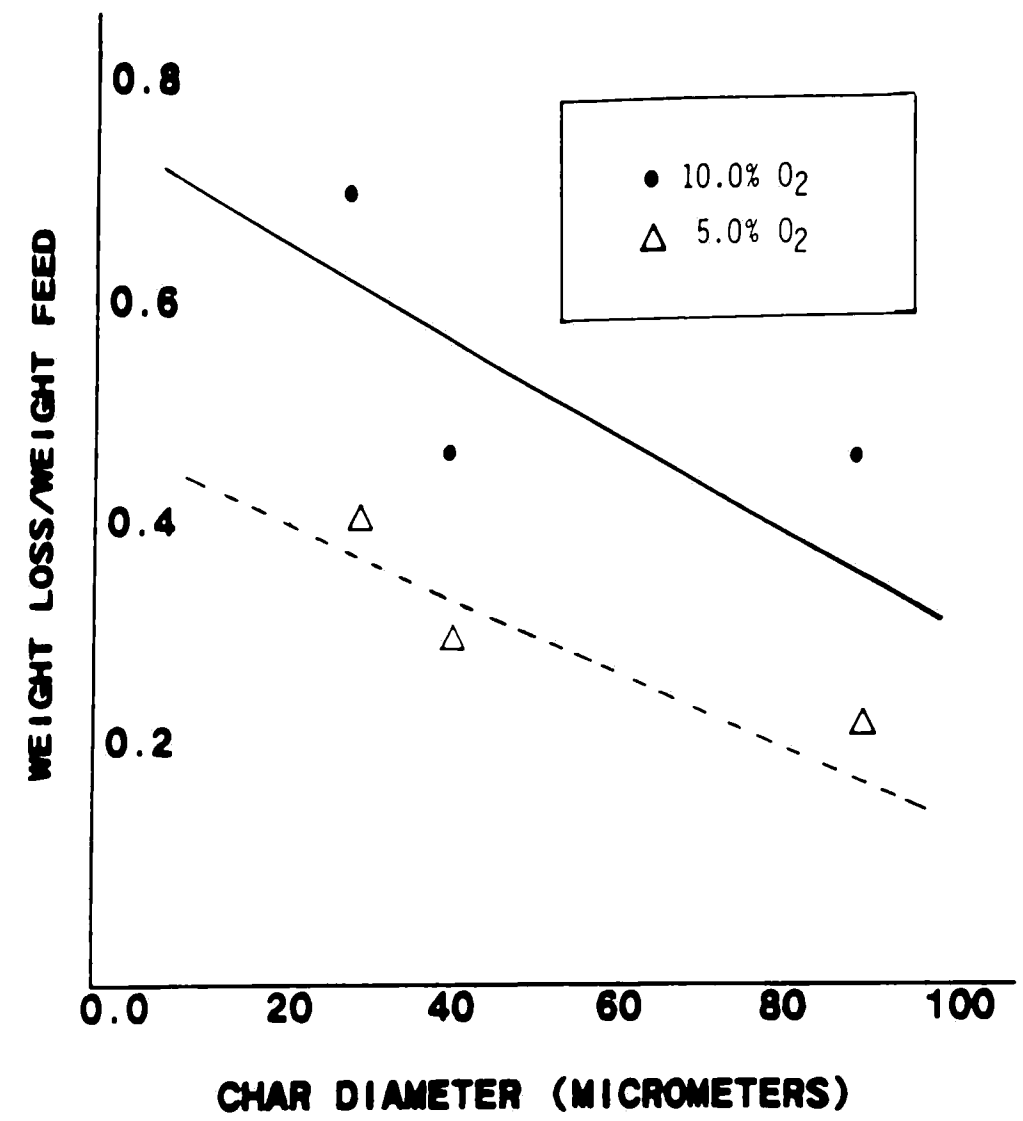


Figure 19. Char Burnout Time Versus Particle Size at 1620°K and 1420°K

Similarly, the char oxidizes more rapidly in an oxygen-enriched environment. These trends are observed because the oxidation reactions are diffusion controlled, depending on the area available for mass transfer. Fast reaction rates are favored by the large surface area to volume (mass) ratio characteristic of small particles. Because the energy-release rate is proportional to the oxidation rate, and oxidation rate and volatile-release rate depend on particle size, the temperature distribution and volatile distribution in a furnace will depend on the coal-particle size used. Therefore, the amount of sulfur trioxide generated in a flame is a function of the coal-particle size, due to the species-concentration dependencies and temperature dependencies of the rate-limited reactions from which it forms and decomposes.

5. SULFUR TRIOXIDE MEASUREMENTS IN A COAL-FIRED UTILITY BOILER

During July 1984, a series of measurements was made of sulfur trioxide levels at Potomac Electric's Morgantown Unit Two using a continuous sulfur trioxide monitor marketed commercially by Severn Sciences Limited. The boiler is a 600-megawatt supercritical-pressure unit fired tangentially using pulverized coal.

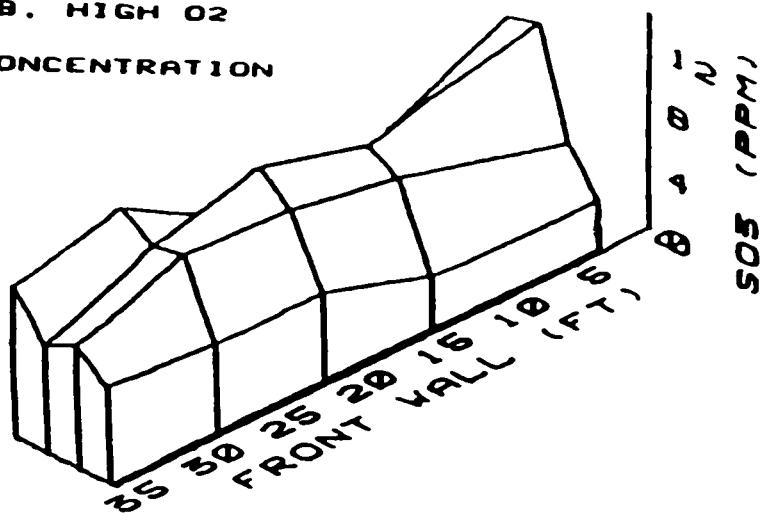
The sulfur trioxide monitor uses an automated isopropyl alcohol absorption technique to measure flue-gas sulfur trioxide concentration. A controlled quantity of flue gas is contacted with a solution of isopropyl alcohol and water. The solution absorbs sulfuric acid and converts gaseous sulfur trioxide to liquid sulfuric acid. The sulfate (equivalent to sulfuric acid) content of this liquid is determined by passing the sulfate-containing solution over barium chloranilate crystals. Each sulfate moiety generates a chloranilate ion, which absorbs light in the UV spectrum. The UV absorbance (535 nm) is measured with a photometer, and the electrical signal sent from the monitor to data logging equipment is converted to equivalent flue-gas sulfur trioxide concentration.

The effect of excess air on sulfur trioxide levels was determined by measuring sulfur trioxide concentrations at the inlet side of the air heater at low (2.2 percent), medium (3.5 percent), and high (5.0 percent) oxygen levels at various locations in the duct. Measurements were made using a grindsize of 85 percent through 200 mesh while unit load was held constant at 480 megawatts. The slag condition was not disturbed by soot blowing during the tests. No attempt was made to establish and correlate pointwise time variations in acid levels.

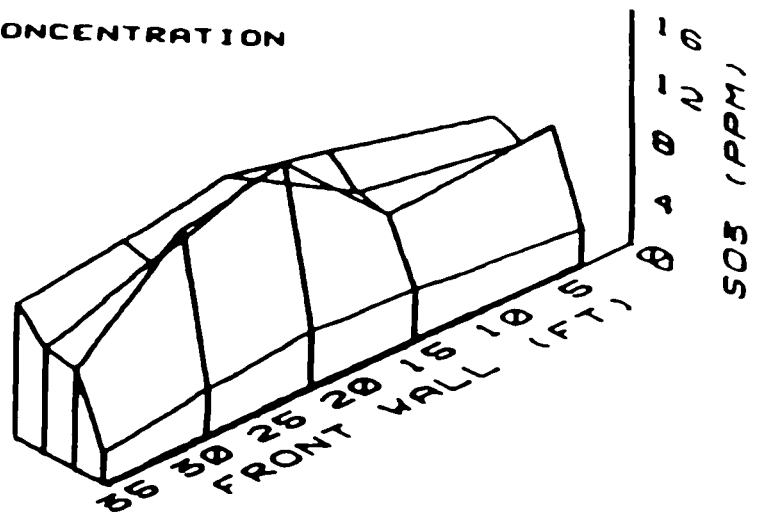
Average sulfur trioxide levels at high, medium, and low oxygen were 8.4, 7.8, and 4.1 ppm respectively. The concentrations were noticeably lower during low-excess-air operation, although there was not a noticeable difference between the sulfur trioxide levels during medium and high-oxygen firing. Representations of the measured distributions are shown in Figure 20. The location of a measured value along the duct wall is labeled in Figure 20, but the penetrations of two, four, six, and eight feet from the front wall are not labeled. The height of a point above the x-y plane is indicative of the value at that position. Generally, acid levels were much lower along the front wall. Also, sulfur trioxide concentrations close to the front wall were not as sensitive to oxygen level as were concentrations in the back of the duct.

The behavior of sulfur trioxide levels with oxygen can not be attributed to one particular source. A decrease in sulfur trioxide could be the result of reduced contact between catalytic surfaces and oxygen, reductions in flame-generated acid, or both. It is also evident that the contributing parameter varies throughout the duct and perhaps with operating condition.

DUCT B. HIGH O<sub>2</sub>  
SO<sub>3</sub> CONCENTRATION



DUCT B. MEDIUM O<sub>2</sub>  
SO<sub>3</sub> CONCENTRATION



DUCT B. LOW O<sub>2</sub>  
SO<sub>3</sub> CONCENTRATION

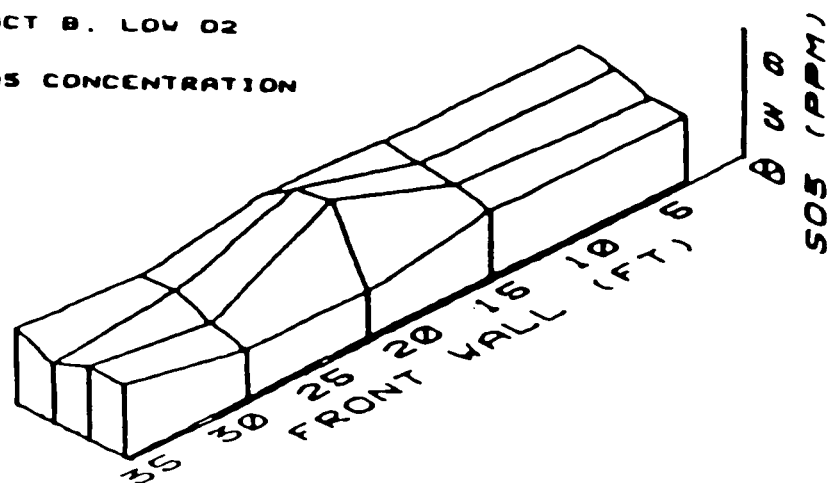


Figure 20. Sulfur Trioxide Profiles Measured at Three Oxygen Levels in a Pulverized-Coal-Fired Utility Boiler

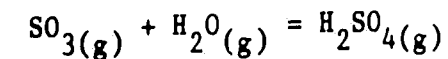


## 6. DEPOSITION PROCESSES

The mixture of sulfuric acid, water, fly ash, and corrosion products can be found in the colder layers of most regenerative air preheaters. The sulfuric acid and water condense simultaneously from the noncondensable components in the flue gas. The sulfuric acid originates from the sulfur trioxide formed in the furnace, while the moisture originates from the primary combustion reactions and from moisture contained in the combustion air. The condensed acid layer traps fly-ash entrained in the gas stream. The dynamics of the heat-transfer processes in the air heater and the operational history of the boiler dictate the magnitude and location of deposits.

### 6.1 The Formation and Deposition of Sulfuric Acid

Sulfuric acid vapor in the gas phase is formed by the combination of sulfur trioxide and water according to the reaction:



It is possible to calculate equilibrium conversion as a function of temperature from the Gmitro and Vermeulen<sup>23</sup>  $K_p(T)$  relationship for this reaction. The manipulations used are as follows:

$$K_p(T) = \frac{P_{\text{SO}_3} \times P_{\text{H}_2\text{O}}}{P_{\text{H}_2\text{SO}_4}}$$

$K_p(T)$  = equilibrium constant given as a power series in temperature.

$P$  = partial pressure of components

$X$  = fractional conversion =  $P_{\text{H}_2\text{SO}_4}/P_{\text{tot}}$

$P_{\text{tot}}$  =  $P_{\text{H}_2\text{SO}_4} + P_{\text{SO}_3}$

$$X = \frac{P_{\text{H}_2\text{O}}}{K_p + P_{\text{H}_2\text{O}}}$$

The resulting plot of conversion versus temperature for a gas containing six percent water vapor is presented in Figure 21.

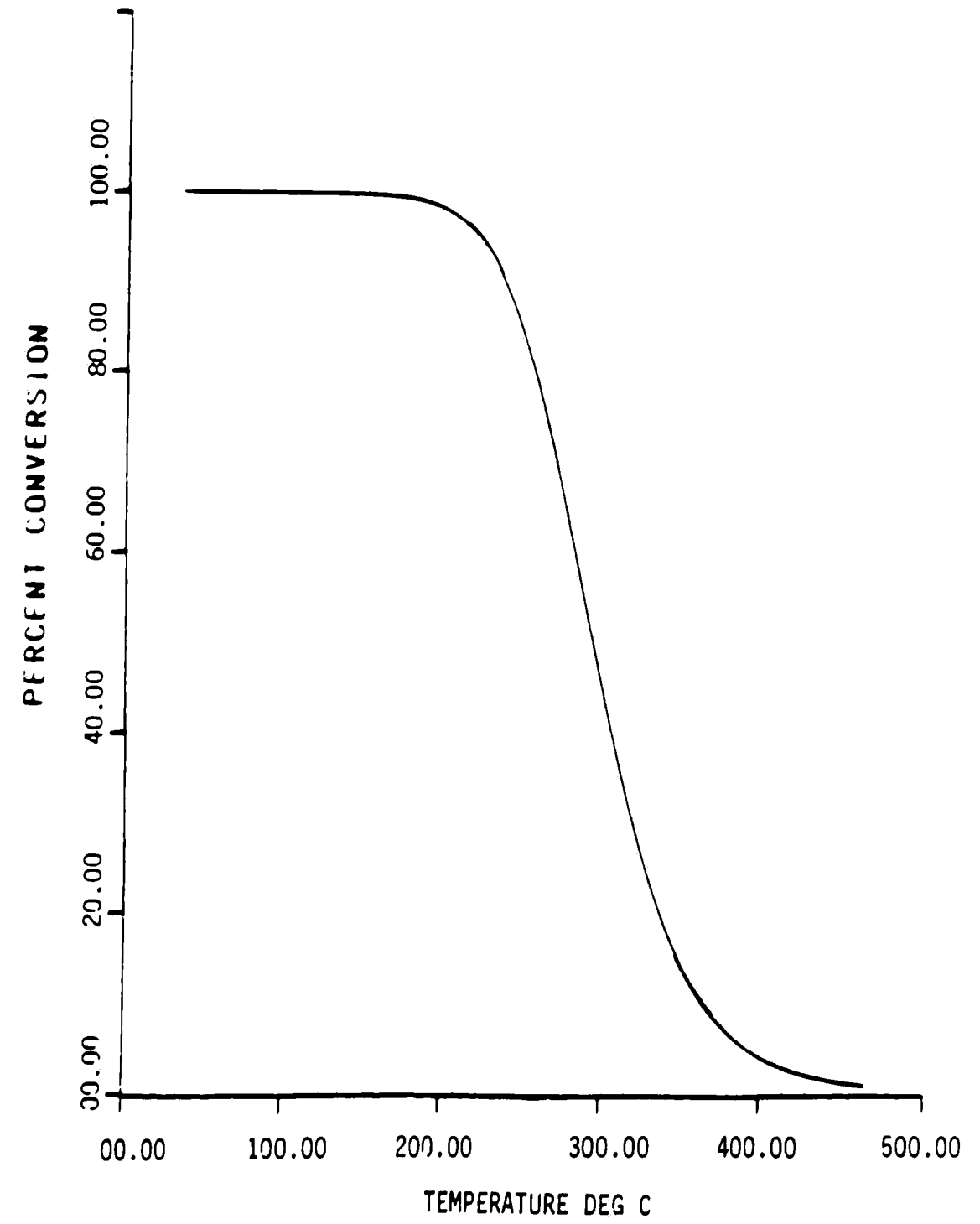


Figure 21. Equilibrium Conversion for the Reaction  $\text{SO}_3 + \text{H}_2\text{O} = \text{H}_2\text{SO}_4$

According to equilibrium, when the flue gas reaches the colder sections of the air heater where acid condensation begins (less than 200°C), essentially all of the sulfur trioxide has combined with water to form sulfuric acid. The rate of this reaction is faster than the gas diffusional rate, so the equilibrium conversion is attained if mixing is complete.<sup>24</sup>

Condensation of a mixture of sulfuric acid and water from flue gas onto a surface is possible once the surface temperature is at or below the saturation (or dewpoint) temperature of the condensing components. The dewpoint temperature is set by thermodynamics, depending on the sulfuric acid concentration and water concentration in the gas. Dewpoint temperatures calculated from the Banchemo correlation<sup>25</sup> in Figure 22 show how dewpoint temperatures decrease as acid levels are reduced and as water levels decrease. The dewpoint temperature is particularly sensitive to the acid concentration in the gas. The compositions of condensed liquids in equilibrium with gases of various acid concentrations were calculated from the Abel<sup>26</sup> and Greenwalt<sup>27</sup> correlations. The results, which appear in Table II, show that the acid concentration in the liquid is more sensitive to the concentration of the acid in the vapor at the lower (vapor acid) concentrations.

The characteristics of sulfuric acid and water condensation from a clean (particle free) carrier gas were demonstrated in the laboratory by Taylor.<sup>28</sup> In his experiments, sulfuric acid and water were vaporized in an evaporator, mixed with air, and drawn through a controlled-temperature pyrex tube. The air flowrate and tube diameter were such that laminar flow prevailed throughout the condenser.

Figure 22. Thermodynamic Dewpoint as a Function of Sulfuric Acid Concentration

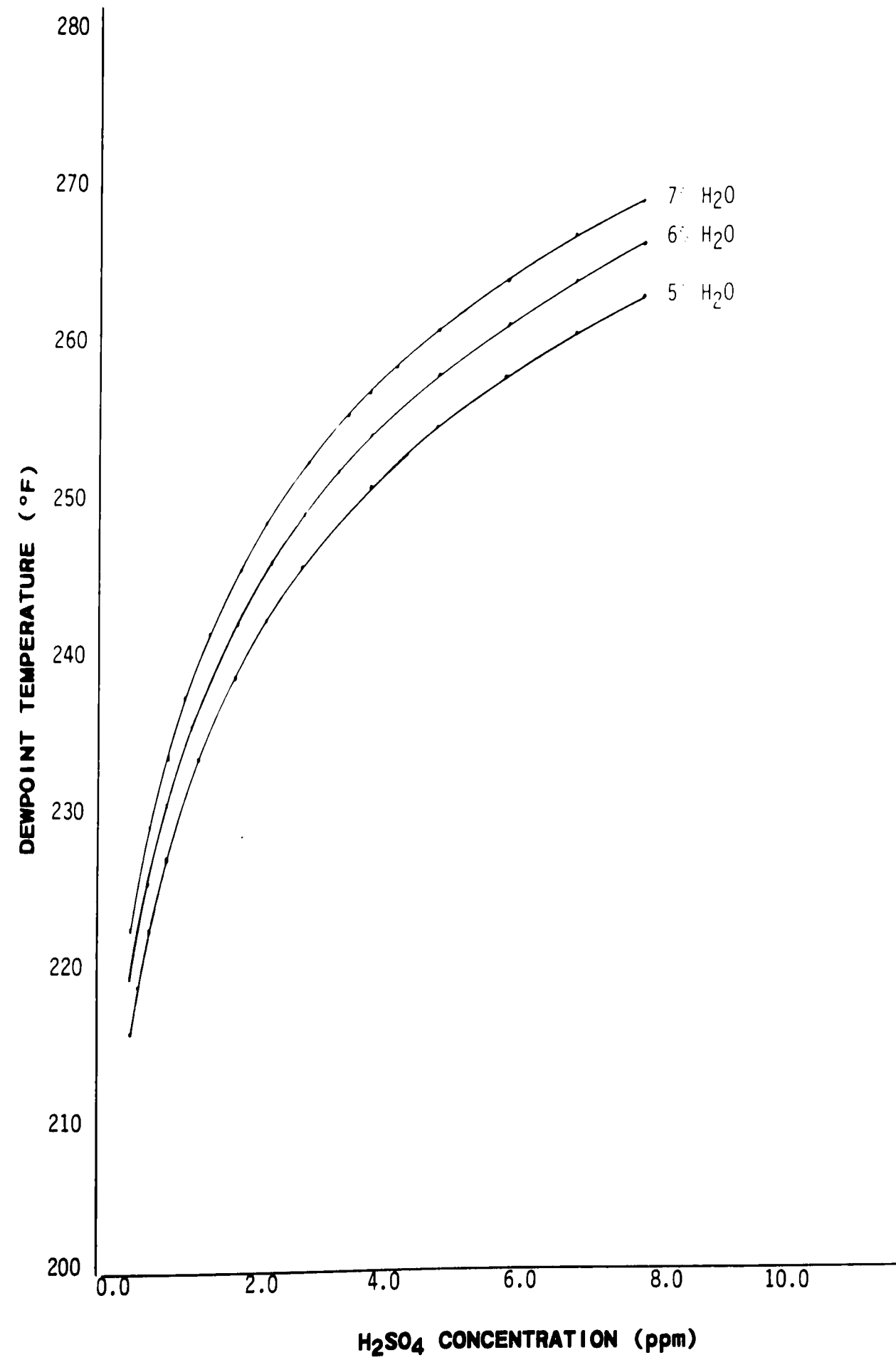


Table II. Composition of Condensed Liquid  
with Various Gas H<sub>2</sub>SO<sub>4</sub> Levels.  
7.5 Percent Water Vapor 1 Atm.

Vapor Volume Fraction (PPM) H <sub>2</sub> SO <sub>4</sub>	Liquid Weight Percent H <sub>2</sub> SO <sub>4</sub>
2.5	80.63
5.0	81.47
7.5	81.93
10.0	82.24
15.0	82.67
20.0	82.97
30.0	83.40

The rate of acid condensation as a function of surface temperature was measured over the range of vapor concentrations encountered in an oil-fired utility boiler. Taylor's results for a synthetic flue gas containing 7.5 percent moisture by volume are presented in Figure 23. The experiment demonstrated how the flux of condensing acid increases as the surface is cooled below the dewpoint temperature. In addition to demonstrating the relationship between surface temperature and acid flux, the results show how reducing acid levels in the vapor decreases the rate of acid condensation for any given temperature difference between the bulk gas and the surface. At temperatures far below the initial condensation temperature, the flux of acid reached a maximum. Upon further reduction of the surface temperature, the acid flux decreased. Flint and Kear<sup>29</sup>, and Rylands and Jenkinson<sup>30</sup> observed this behavior in similar experiments. The Rylands and Jenkinson apparatus permitted visual observation of the condensation process. Rylands and Jenkinson observed film-type condensation on the walls of the condenser, and reported that mist was entrained in the gas stream in the zone of diminished-condensation.

The observed behavior can be rationalized by examining the heat and mass-transfer processes occurring. In order for the condensable components in a system to condense, concentration gradients must exist in the gas between the bulk gas and the surface. If the condensable components are relatively dilute, the bulk-flow of material to the surface is negligible, and the condensable compounds move to the surface by diffusion along the concentration gradients.<sup>31</sup> As the surface temperature is reduced, the gas-side interfacial concentrations

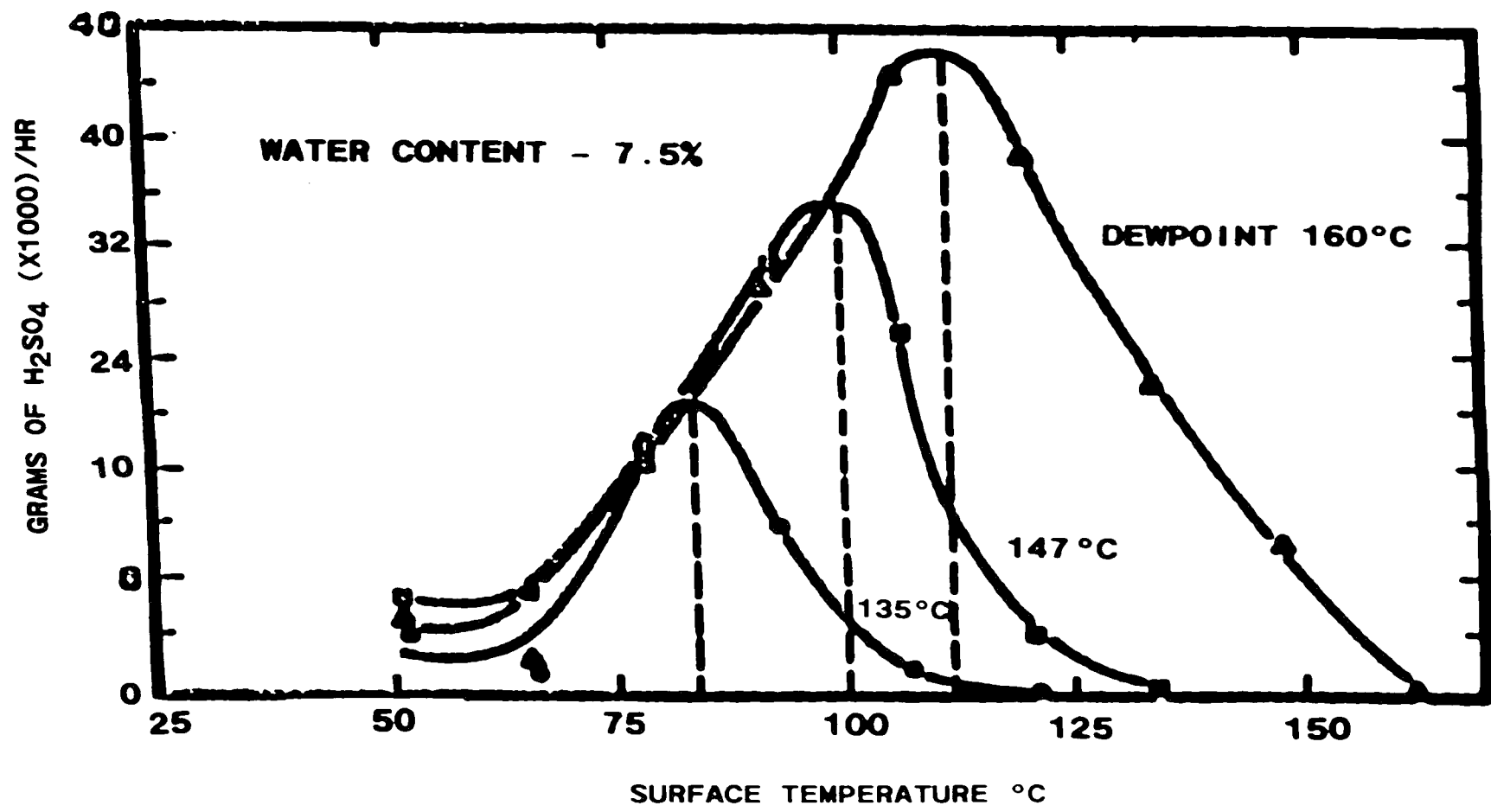


Figure 23. Condensation Rate Versus Surface Temperature and Vapor-Dewpoint Temperature

of the condensable materials are reduced, thereby increasing the concentration gradients, with a concomitant increase in condensation rate.

A temperature profile also develops between the bulk gas and the cooled surface. Heat transport occurs by convection and by movement of thermal energy carried by the migrating species. Thermodynamics sets the maximum allowable acid concentration at positions throughout the gas according to local temperature and local concentrations of sulfuric acid and water. At positions where local vapor concentrations exceed those permitted by the local temperature, the gas either supersaturates or nucleates to form liquid droplets. The amount of supersaturation tolerated by the gas will affect the concentration gradients, which in turn will affect the condensation rate. The reduction in acid flux resulting in extensive surface subcooling is likely attributed to reductions in the concentration of acid in the vapor phase due to the formation of deposition-resistant liquid droplets.

Because the condensable components are convected with the bulk-gas flow, and because convection parallel to the surface affects the concentration gradients, the gas-flow characteristics are expected to interact with the condensation rate behavior.

#### 6.2 Ash and Liquid-Droplet Deposition

Ash particles of various sizes enter the air preheater with the flue gas. These particles can deposit onto the surfaces of the air preheater passages by a variety of physical processes. The operative process depends on particle characteristics (principally size) and the flow characteristics of the gas stream. Ash deposition occurs on surfaces which are both above and below the acid-dewpoint temperature.



Although the mechanisms of deposition are similar in both regions, the magnitude and effect on air-heater performance is different.

The motion of very-small solid particles in a gas stream occurs by Brownian motion. Brownian motion affects particles appreciably smaller than 1000 angstroms. The transport of these particles results from collisions with gas molecules and other solid particles. Therefore, the particles diffuse from areas of high concentration to low concentration, as do gases. The smallest particles comply to the equations governing molecular diffusion.<sup>32</sup>

The movement of larger particles in a gas stream with diameters of up to one micron are dominated by the path of the gas stream. Ash particles in this size range are also subject to Brownian motion.

Particles larger than one micron can only be transported to a surface perpendicular to the reaction of flow by turbulent diffusion processes. These particles impact a surface when kinetic energy imparted to them by gas eddies propell them to the surface. Turbulent diffusion is associated exclusively with turbulent flow, which is characterized by the presence of eddies.

Frieland and Johnstone<sup>35</sup> found that no ash-type solids deposited in the entrance region of a pipe when the Reynolds number based on pipe diameter was kept below 4000, with particles in the size range of 0.80 to 2.63 microns.

A plot of solid deposition rate as a function of surface temperature measured at an oil-fired boiler downstream of the air preheater is shown in Figure 24.<sup>34</sup> Above the acid condensation temperature, solid accumulation occurs at a noticeable rate. Below the condensation temperature solids accumulate at a much faster rate (note

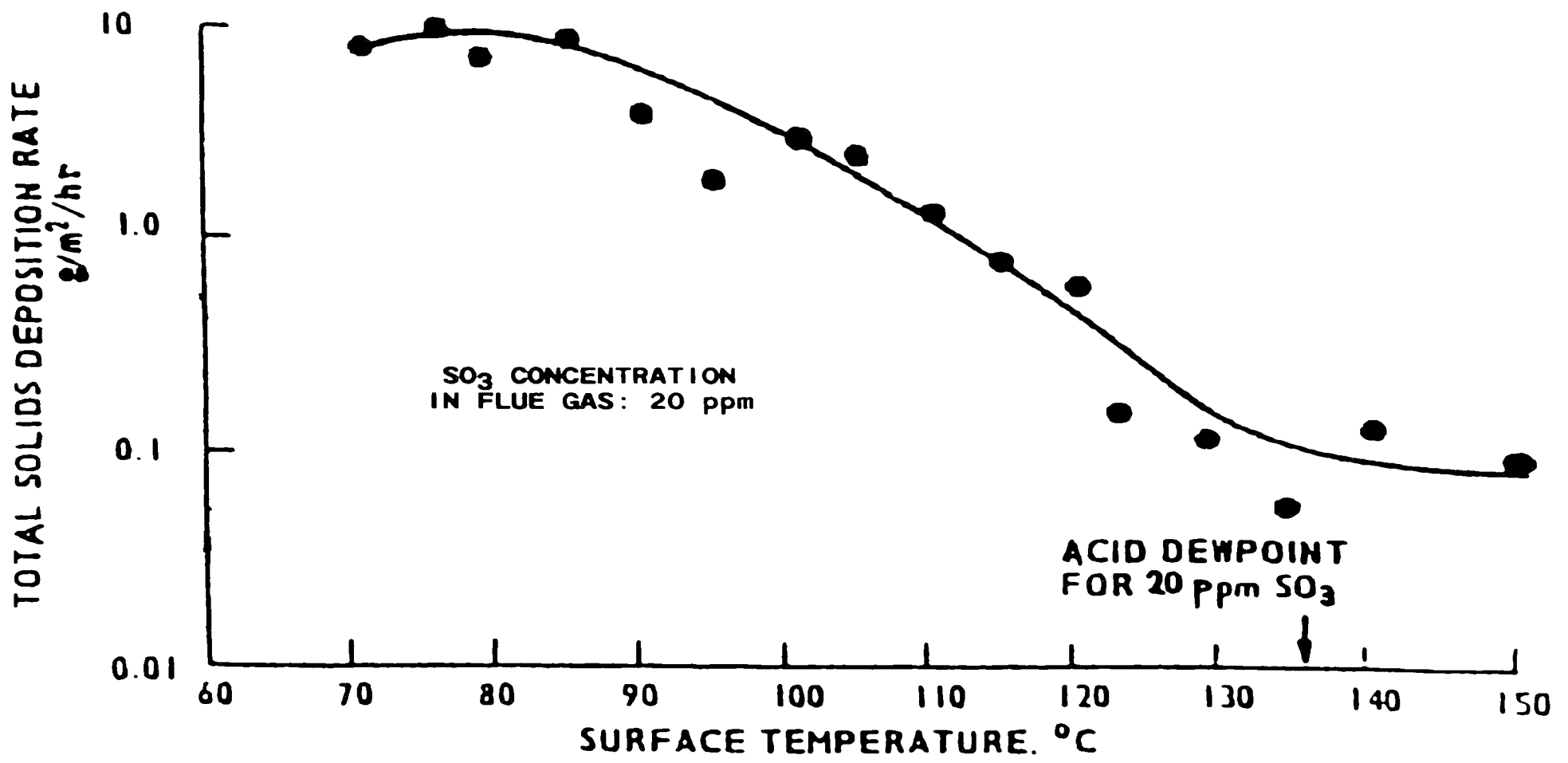


Figure 24. Solid Deposition Rate Temperature Dependence

the log scale). Although particle migration to the surface in the condensation and non-condensation zones are similar, the agglomeration of sulfuric acid, water, corrosion products, and fly ash in the condensation zone is more resistant to mechanical dislodging than agglomerates in the non-condensation zone. Therefore, enhanced accumulation rates and less friable deposits are found in the condensation region.

### 6.3 Acid Condensation Interference by

#### Particles Entrained in the Gas Stream

Whitingham<sup>35</sup>, Flint<sup>29</sup>, and Kear<sup>36</sup> determined the effect of carbon smoke addition on dewpoint. Meter behavior using flue gases generated by a laboratory facility. The flue gas was generated with a fully-aerated Bunsen flame by combusting coal gas. The flame was housed in a pyrex chimney with side arms for gas sampling located well above the visible flame. Desired sulfur trioxide levels were established by directly adding sulfur trioxide (obtained from the oxidation of sulfur dioxide with oxygen over a catalyst), or by adding sulfur dioxide to the primary coal-gas supply. Carbon smoke was produced in and above the Bunsen flame by the partial combustion of an auxiliary gas supply. The smoke concentration was determined by weighing the amount of material deposited on a water-cooled tube exposed to the flame gases.

A dewpoint meter consists of a glass thimble carrying a thermocouple and two electrodes across which an electrical potential is applied. The glass element is exposed to the flue gases while cool air is directed against the backside of the thimble at a rate which establishes the desired temperature. The presence of sulfuric acid

solution on the detector is indicated by the flow of current across the electrodes. Current flow is monitored by a remote amp meter. The measured conductivity depends on the thickness of the condensed film and the conductivity of the deposited material. The dewpoint is obtained by cooling the probe to the point where current flow is present and steady.

The hot products of combustion were drawn over the glass thimble of a dewpoint meter by a vacuum pump. Measurements were made of the dewpoint temperature and the conductivity versus time behavior associated with operation below the acid-dewpoint temperature. The dewpoint temperature did not change as the concentration of carbon smoke increased from zero to 0.14 mg/liter. The rate of increase in conductivity ten degrees Celcius below the dewpoint was determined with carbon smoke removed from the gases and found to vary linearly with time (a result of the steady increase in condensed-film thickness). When carbon smoke was introduced at a rate of 0.14 mg/liter, there was a substantial reduction in the rate of conductivity increase as shown in Figure 25.

The sulfuric acid content of the gas mixture was simultaneously measured using the isopropyl alcohol absorption technique. The analysis was conducted such that the sum of the acid in the gas phase and acid loosely associated with the carbon smoke was measured. Little change in acid level occurred with up to 0.14 mg/liter of smoke addition, although substantial reductions resulted with higher smoke burdens. Therefore, the amount of gas-phase acid remained constant with moderate carbon-smoke addition, because both the total acid level and the dewpoint-meter dewpoint remained unchanged.

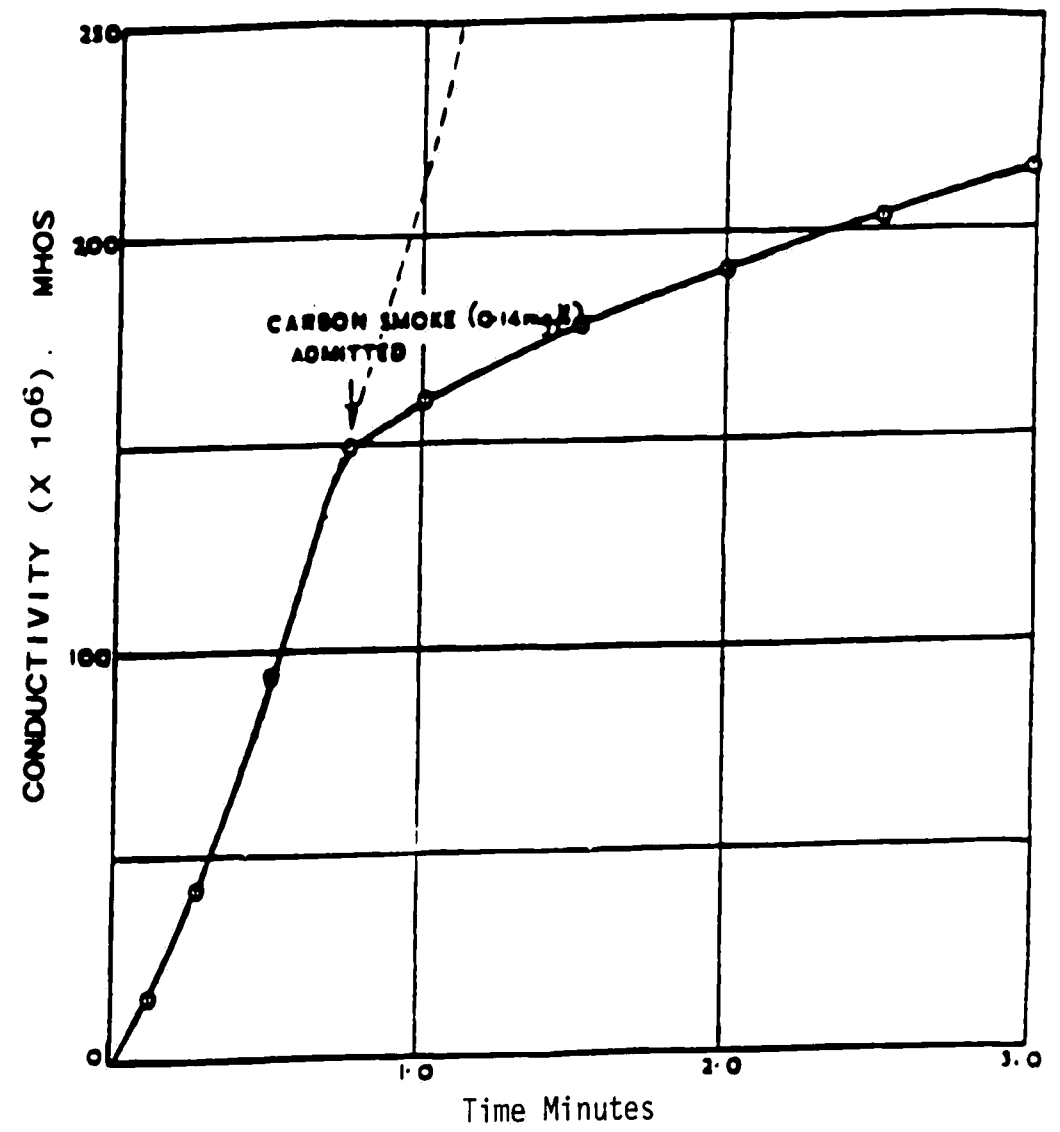


Figure 25. Effect of Carbon Smoke Addition on Dewpoint-Meter Conductivity-Rate Behavior Ten Degrees Centigrade Below the Instrument Dewpoint

The authors attributed the reduction in conductivity rate to reductions in the deposited acid layer conductivity resulting from chemical reactions between the acid deposit and the observed carbon-smoke deposit. It is suggested here that the carbon ash could also have reduced the acid-deposition rate by reducing the amount of acid in the vapor through acid-mist formation.

The effects of ash entrained in boiler flue gases on condensation behavior was also investigated by Corbett and Flint.<sup>37</sup> Two stoker-fired boilers were adapted to auxiliary pulverized-coal firing in an attempt to impart the lower corrosion potential associated with pulverized-coal firing to the stoker-fired units. With the modifications, 20 percent of the full-load fuel requirement could be met by pulverized coal.

At the first site, measurements of sulfur trioxide levels at the economizer exit using the isopropyl alcohol/water absorption technique indicated a negligible reduction in acid level with auxiliary pulverized-coal firing. The dewpoint temperature at this location measured with a dewpoint meter was not altered by auxiliary firing, although the rate-of-acid buildup curve generated by the device changed dramatically, as shown in Figure 26. Such curves are obtained by monitoring the rate-of-current increase at various temperatures below the condensation-onset temperature. The reduction in current rate associated with the pulverized-coal firing can be attributed to a reduction in the conductivity of the material depositing on the detector element and/or a decrease in the actual acid condensation rate.

Similar measurements were made at an alternate site. This unit experienced no change in sulfur trioxide level or dewpoint-meter

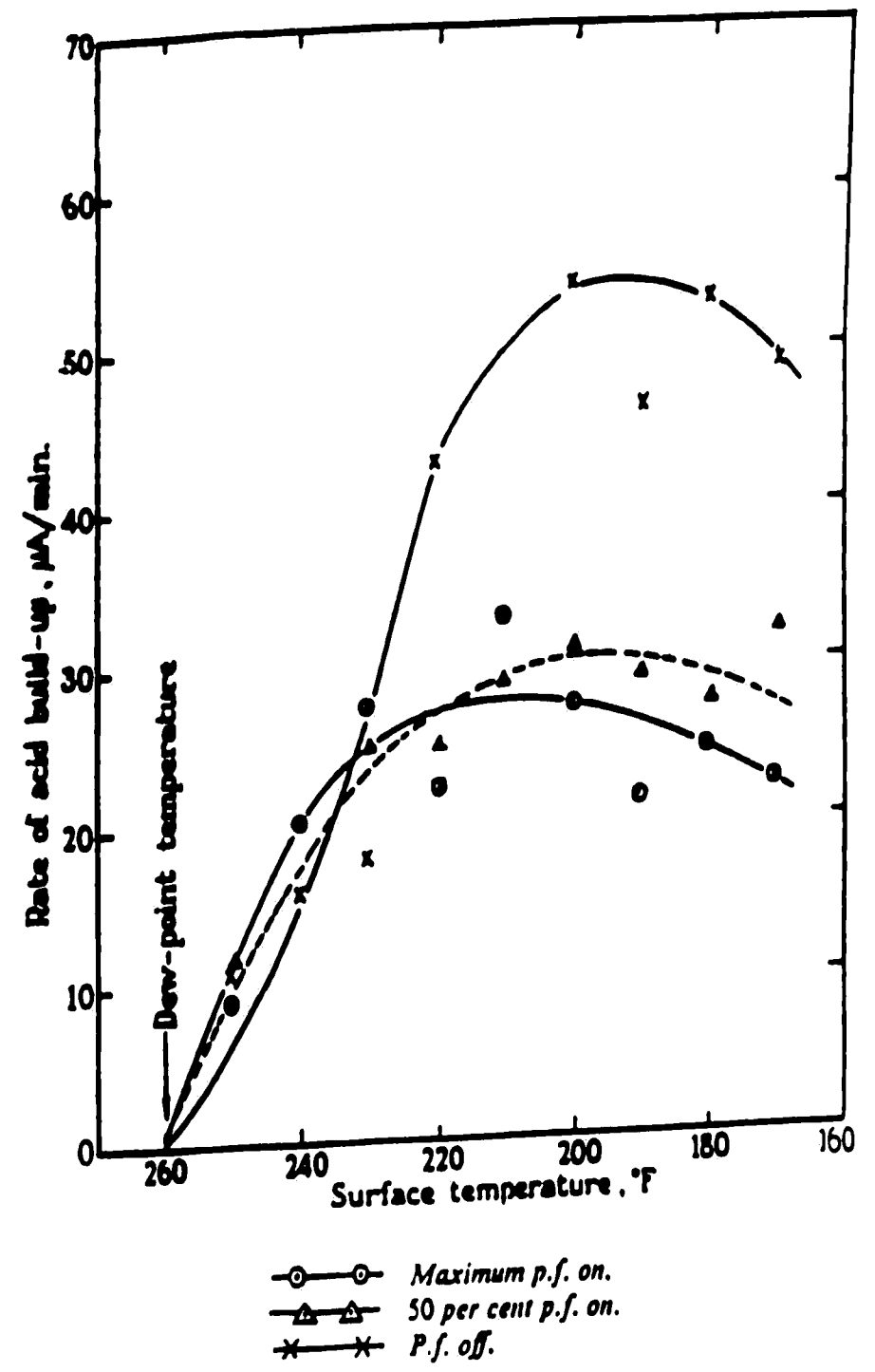


Figure 26. Effect of Auxiliary Coal Firing on the Current-Rate Curve of a Stoker-Fired Utility Boiler

dewpoint temperature with auxiliary firing. To complement these experiments, acid-deposition rate was measured as a function of surface temperature by exposing a controlled temperature surface to the flue gases for a set time, followed by quantitative determination of the unbound sulfate (sulfuric acid) content in the deposit. The rate of acid condensation was reduced with auxiliary pulverized-coal firing, as shown in Figure 27. The magnitude of the effect depended on the surface temperature.

To determine if the observed phenomena resulted from the increased dust burden associated with auxiliary pulverized-coal firing, dust collected from an electrostatic precipitator of a pulverized-coal unit was manually introduced at the inlet of the secondary air fan while operating without auxiliary firing. Dewpoint-meter dewpoint temperatures were monitored, and rate-of-current-buildup measurements were made 6 Fahrenheit degrees below the instrument dewpoint. The results displayed in Figure 28 show that modest dust feed rates had no effect on dewpoint-meter dewpoint temperature, although the conductivity rate decreased. More significant dust burdens reduced the onset temperature below the limit of detectability of the dewpoint meter.

The evidence presented suggests that the presence of particles in the gas stream reduces the acid condensation rate onto a surface cooled below the condensation onset-temperature. However, condensation rates inferred from dewpoint-meter current rates may be obscured by changes in the conductivity of the condensed acid due to chemical and/or physical changes associated with simultaneous dust deposition.

The mode of interaction between the particles and the condensation



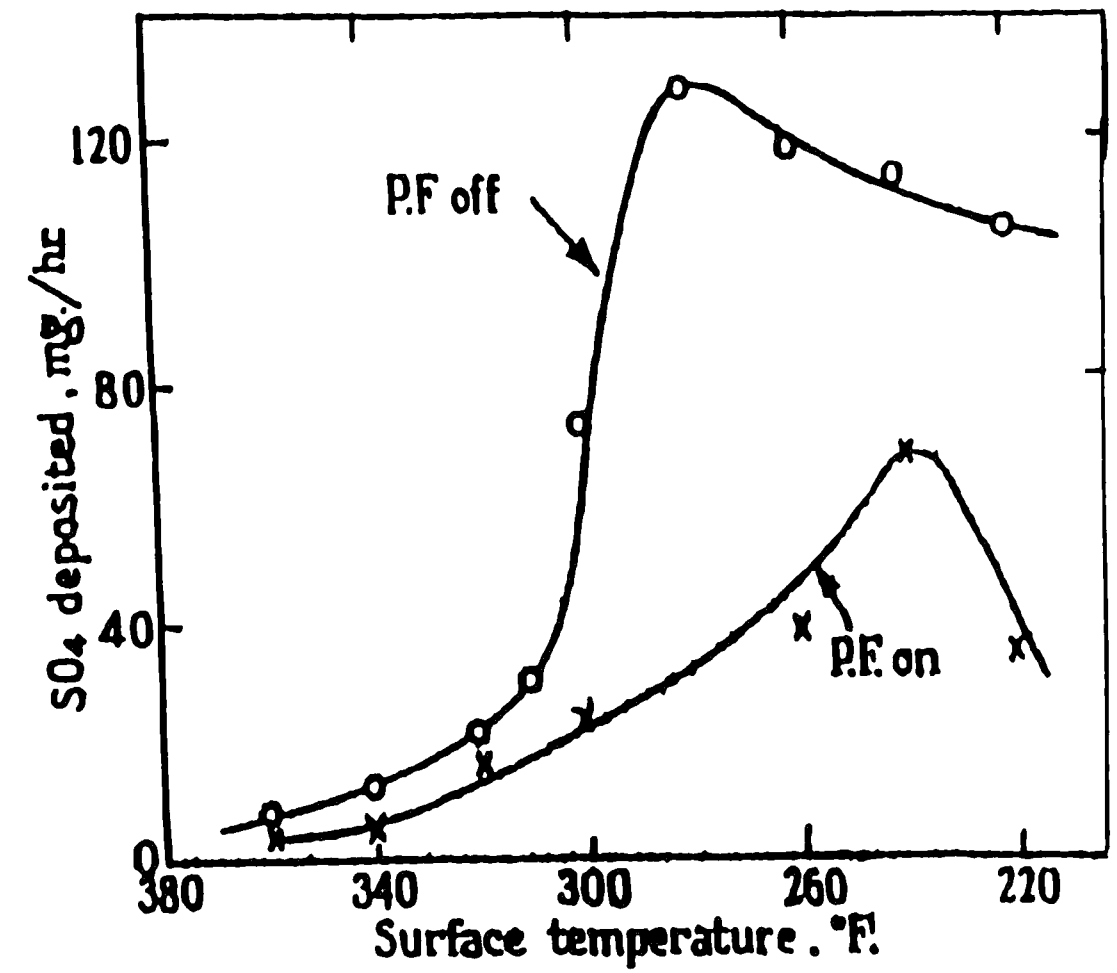


Figure 27. Effect of Auxiliary Coal Firing on the Sulfuric Acid Deposition-Rate Profile at the Duct Wall of a Stoker-Fired Utility Boiler

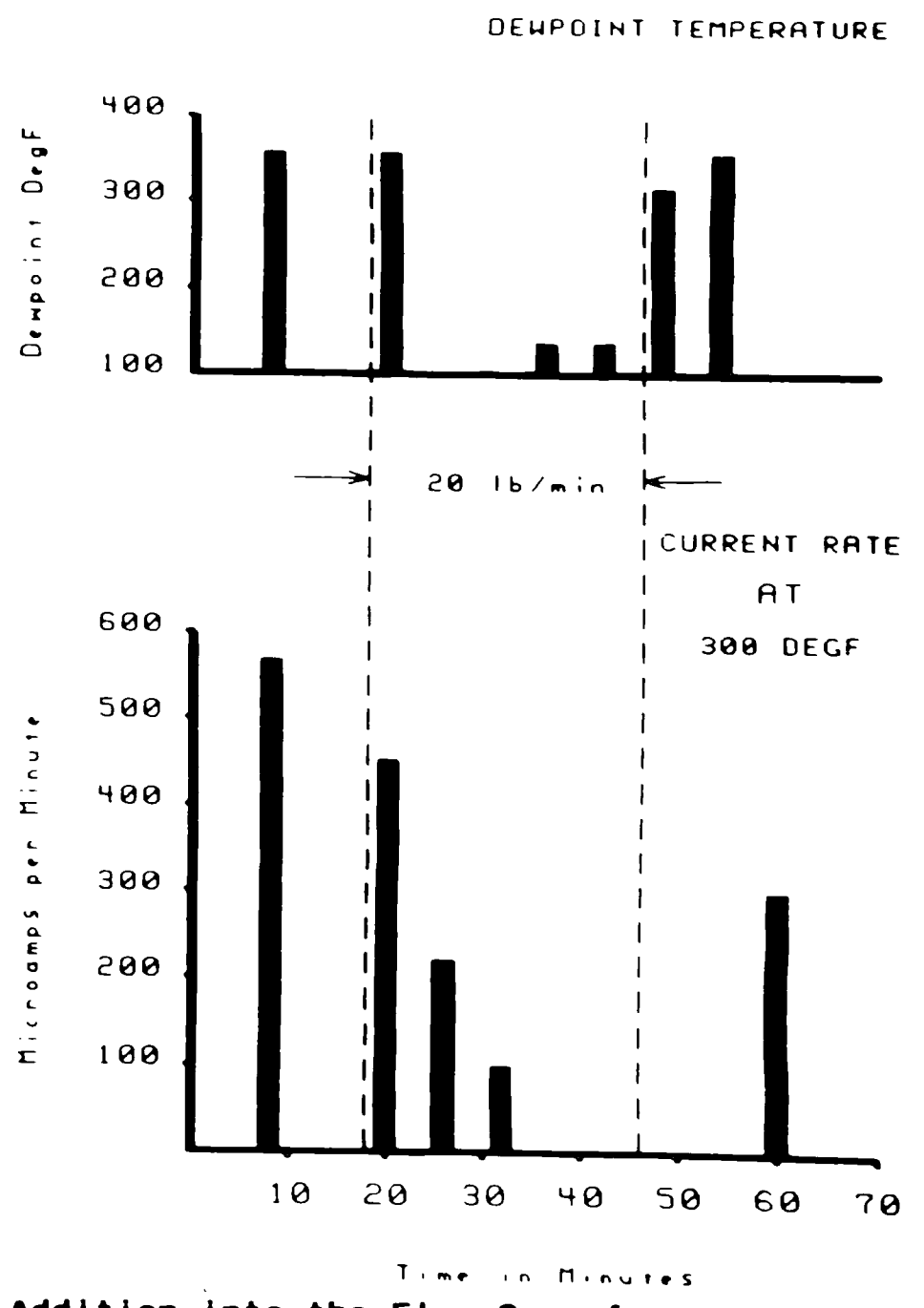
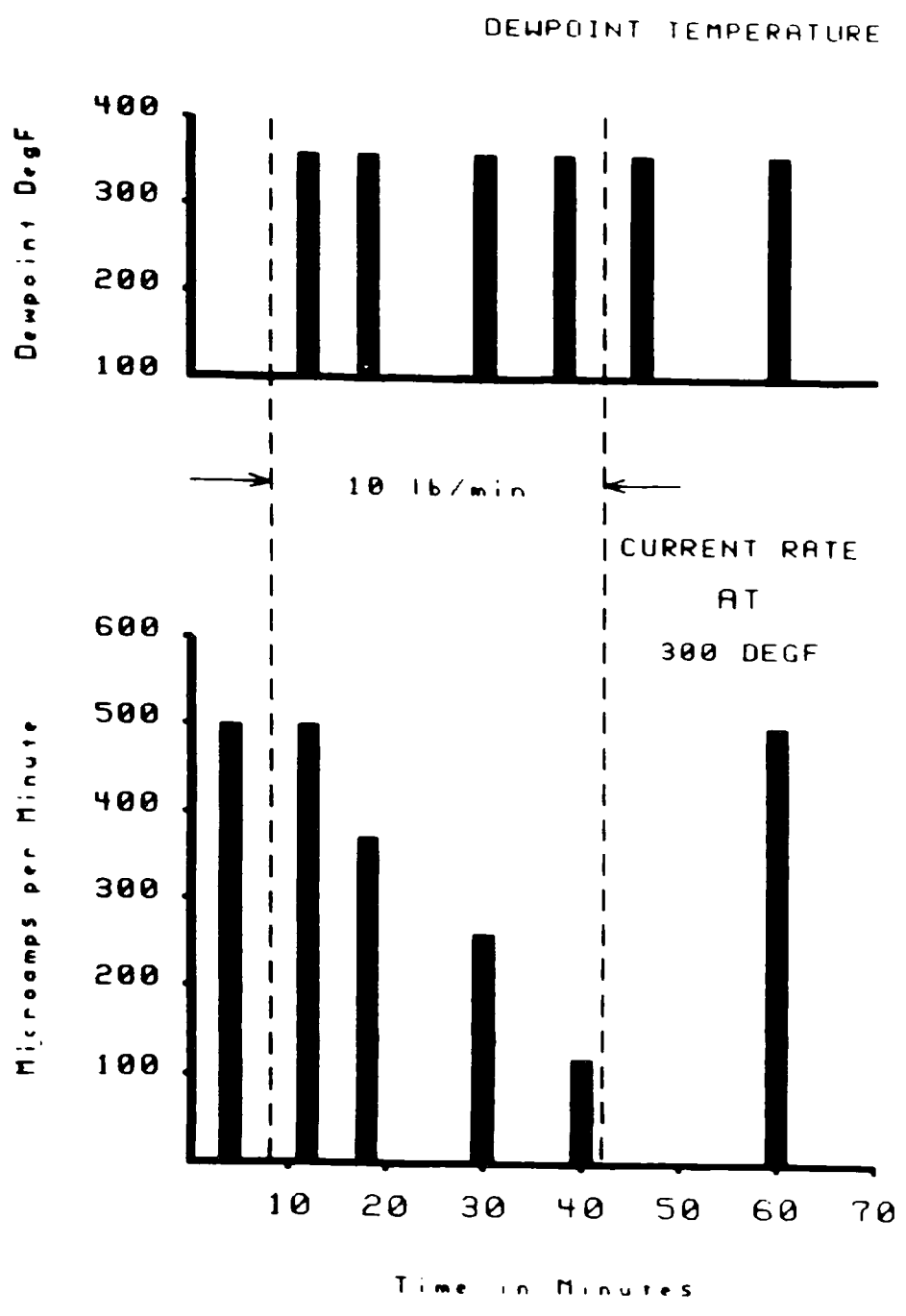


Figure 28. Effects of Ash Addition into the Flue Gas of an Oil-Fired Boiler on Dewpoint Meter Behavior

process remains to be determined. Three mechanisms are suggested.

1. Supersaturation reduction by enhanced nucleation

If the gas above a cooled surface is locally supersaturated before particle addition, the addition of particulate material would reduce supersaturation by increasing the rate of liquid-droplet formation. This mist formation would reduce the molecular-diffusion rate of acid to the surface by reducing the acid-concentration gradient in the vapor between the bulk and the vapor-liquid interface.

2. Local adsorption by solid particles

In general, the adsorption capacity of solid material such as carbon is greater at lower temperatures. As particles approach a cooled surface, they see a cooler environment. Such particles might absorb vapors such as sulfuric acid and water, reducing the concentrations of these components in the vapor.

3. Momentum transport modification

The velocity profile of a gas flowing through a conduit is a function of radial and axial position. If a solid particle entrained in a gas stream was large enough such that it experienced a non-symmetrical velocity field, the particle would spin and translate. Because momentum, heat, and mass-transport rates are interrelated, the mixing caused by solid particles in a flowing gas stream could modify mass-transfer (condensation) rates.

#### 6.4 Dynamics of Deposition in the Air Heater

The nature of fouling, plugging and ultimately corrosion in the regenerative air heater is dependent upon the interrelationship between basket-metal temperatures and the dynamics of the condensation processes.

For the design case a regenerative air heater operates with constant flow rates and temperatures on the gas and air sides. Temperature gradients in the metal in both the flow direction and the rotational direction are expected. Figure 29 shows simulated metal temperature distributions for the cold-end layer of the metal basket on the gas side at two positions in the rotational arc. The curve with the lower temperature represents metal that has just entered the hot gas stream, while the curve with higher temperatures is for the metal at the end of its path in the gas stream.

Consider a flue gas with an acid dewpoint of 215°F flowing over the surface at these positions. Just as the metal basket enters the flue gas duct from the cold-air duct (lower curve on Figure 29), acid condensation would occur everywhere on the surface because metal temperatures are below the condensation point throughout, and a zone of diminished condensation and mist formation would develop downstream of the initial condensation point. At the end of its travel in the flue-gas duct (upper curve on Figure 29), condensation would occur only at the very end of the basket. Furthermore, if the acid that condensed on the surface at its first exposure to the gas stream did not react on the surface, it might well evaporate at this stage. If the magnitude of the deposition and evaporation rates are significant, higher sulfur trioxide levels would be observed at the gas outlet on one side of the duct.

Fly-ash deposition can occur on all exposed surfaces of the air heater

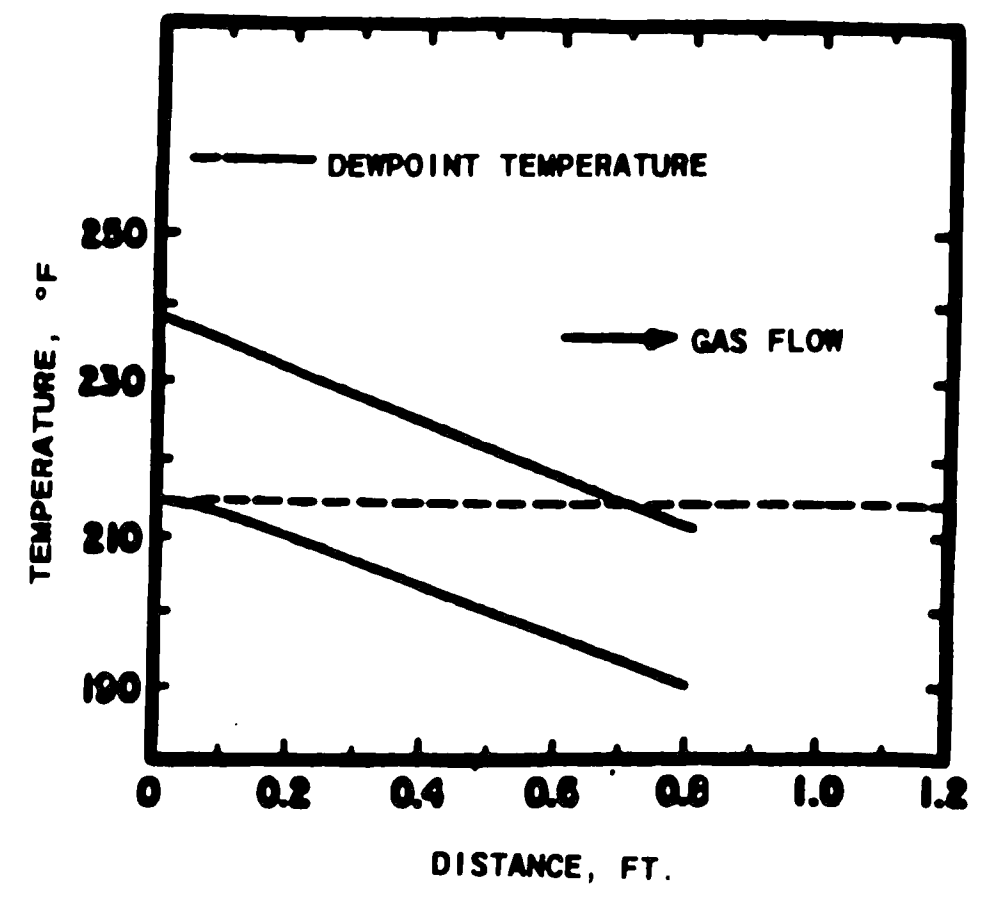


Figure 29. Simulated Gas-Side Air-Heater-Basket Metal Temperatures (Coal End, Distributions at Inlet and Outlet)

as previously described. The deposits are subject to repeated cooling by inflowing combustion air and further deposition during exposure to flue gas. Soot blowing of the air heater removes the more friable material, but the temperatures associated with steam soot blowing can further reinforce the structure of cemented material in the condensation zone. Therefore, the deposits on basket metal surfaces are the result of condensation, evaporation, and reaction of condensate with basket metal. The magnitude, location and effect of the deposits are dictated by the dynamics of the heat-transfer processes in the air heater and the operational history of the boiler.

## NOMENCLATURE

°C	=	degrees Celcius
cm <sup>3</sup>	=	cubic centimeters
ft	=	feet
gmol	=	gram moles
>	=	greater than
hr	=	hours
°K	=	degrees Kelvin
k <sub>1</sub>	=	kinetic rate parameter
M	=	chemically inert molecular component
μA	=	microamp
μm	=	micrometer
mg	=	milligram
msec	=	millisecond
min	=	minutes
ppm	=	parts per million
pf	=	pulverized coal fired
%	=	percent
hν	=	radiation of energy
STP	=	standard temperature and pressure
wt	=	weight

## SUPERSCRIP

*	=	activated species containing additional vibrational, rotational, or translational energy
°	=	degrees

#### REFERENCES

1. Hedley, A. B., Paper II of The Mechanism of Corrosion by Fuel Impurities. Ed. Johnson and Littler, Butterworths, London, p. 204, (1963).
2. Lewis, B., and Von Elbe, G., Combustion, Flames, and Explosion of Gases. Academic Press, New York, p. 78, (1951).
3. Levy, A., and Merryman, E. L., "SO<sub>3</sub> Formation in H<sub>2</sub>S Flames", Journal of Engineering for Power, Transactions of the ASME, Series A, vol. 87, pp. 374-378, (1965).
4. Dooley, A., and Whittingham, G., "Oxidation of Sulphur Dioxide in Gas Flames", Transactions of the Faraday Society, 42, p. 354, (1946).
5. Whittingham, G., "The Oxidation of Sulphur Dioxide in Slow Combustion Processes", Transactions of the Faraday Society, 44, p. 141, (1948).
6. Gaydon, A. G., and Whittingham, G., "The Spectra of Flames Containing Oxides of Sulphur", Proceedings of the Royal Society, 189, p. 313, (1947).
7. Fenimore, C. P., and Jones, G. W., "Sulfur in the Burnt Gas of Hydrogen-Oxygen Flames", Journal of Physical Chemistry, 69-10, p. 3593, (1965).
8. Merryman, E. L., and Levy, A. "Sulfur Trioxide Flame Chemistry - H<sub>2</sub>S and COS Flames", Thirteenth International Combustion Symposium, The Combustion Institute: Pittsburg, p. 427, (1971).
9. Nettleton, M. A., and Stirling, R., "Formation and Decomposition of Sulphur Trioxide in Flames and Burned Gases", Twelfth International Combustion Symposium, The Combustion Institute. Pittsburg, p. 635, (1969).
10. Barrett, R. E., Hummell, J. D., and Reid, W. T., "Formation of SO<sub>3</sub> in a Non-Catalytic Combustor", Journal of Engineering for Power, Transactions of the ASME, Series A, Vol. 7, pp. 165-172, (1966).
11. Manning, G. H., "Communications on Bonded Deposits on Economizer Heating Surfaces and on Causes of High Dewpoint Temperatures in Boiler Flue Gases", Proceedings of the Institute of Mechanical Engineers, p. 151, (1944).
12. Tolly, G., "The Catalytic Oxidation of Sulphur Dioxide on Metal Surfaces. Part I", J.S.C.I., 67, p. 369, (October 1948).
13. Tolly, G., "The Catalytic Oxidation of Sulphur Dioxide on Metal Surfaces. Part II. The Reaction of Sulphur Dioxide and Oxygen at a Mild Steel Surface", J.S.C.I., 67, p. 401, (November 1948).



14. Burnside, W., Marskell, W. G., and Miller, J. M., "The Influence of Superheater Metal Temperature on the Acid Dewpoint of Flue Gases", Journal of the Institute of Fuel, p. 261, (June 1956).
15. Barrett, R. E., "High Temperature Corrosion Studies in an Oil Fired Laboratory Combustor", Transactions of the ASME, Journal of Engineering for Power, p. 288, (1967).
16. Smoot, L. D., and Pratt, D. T., Pulverized Coal Combustion and Gasification, "Mechanisms and Kinetics of Pollutant Formation During Reaction of Pulverized Coal", pp. 183-215, Plenum Press, N.Y., (1979).
17. Solomon, P. R., "The Evolution of Pollutants During the Rapid Devolatilization of Coal", Report R76-952588-2 United Technologies Research Center, East Hartford, Conn., (1977).
18. Yergey, A. L., Lampe, F. W., Vestal, M. L., Fergusson, G. J., Johnston, W. H., Snyderman, J. S., Essenhigh, R. H., and Hudson, J. E., "Nonisothermal Kinetics Studies of the Hydrodesulphurization of Coal", Industrial Engineering Chemistry, Process Design and Develop., Vol. 13, No. 3, 1974.
19. Gronhoud, G. H., Tufte, P. D., and Selle, S. J., "Some Studies on Stack Emissions from Lignite-Fired Powerplants" in Proceedings of Bureau of Mines - University of North Dakota Symposium: Technology and Use of Lignite, pp. 83-102, Report No. IC 8650, U.S. Bureau of Mines, Washington, D.C., (1973).
20. Ely, F. G., and Schueler, L. B., Furnace Performance Factors Supplement to Transactions of ASME, 66, p. 23, (1944).
21. Field, M. A., Gill, D. W., Morgan, B. B., Hawesley, P. G. W., Combustion of Pulverized Coal, The British Coal Utilization Research Association, Letherhead, p. 396, (1967).
22. Field, M. A., "Rate of Combustion of Size Graded Fractions of Char from a Low Rank Coal between 1200°K and 2000°K".
23. Gmitro, J. I., and Vermeulen, T., "Vapor-Liquid Equilibrium for Aqueous Sulfuric Acid", A.I.Ch.E. Journal, p. 740, (September 1964).
24. Goodeve, C. F., Eastman, A. S., and Dooler, A., "The Reaction Between Sulfur Trioxide and Water Vapors in a New Periodic Phenomenon", Transactions of the Faraday Society, 30, p. 1127, (1934).
25. Banchemo, J. T., and Verhoff, F. H., "Evaluation and Interpretation of the Vapor Pressure Data for Sulphuric Acid Aqueous Solutions with Application to Flue Gas Dewpoints", Journal of the Institute of Fuel, p. 76, (June 1975).

26. Abel, E., "The Vapor Phase Above the System Sulfuric Acid-Water", Journal of Physical Chemistry, 50, p. 260, (1946).
27. Greenwalt, C. H., "Partial Pressure of Water out of Aqueous Solutions of Sulfuric Acid", Industrial and Engineering Chemistry, 17, p. 522, (1925).
28. Taylor, H. D., "The Condensation of Sulfuric Acid on Cooled Surfaces Exposed to Hot Gases Containing Sulfur Trioxide", Transactions of the Faraday Society, 47, p. 1114, (1951).
29. Flint, D., and Kear, R. W., "The Corrosion of a Steel Surface by Condensed Films of Sulphuric Acid", Journal of Applied Chemistry, p. 388, (September 1951).
30. Rylands, J. R., and Jenkinson, J. R., "The Acid Dewpoint", Journal of the Institute of Fuel, p. 299, (June 1954).
31. Colburn, A. P., and Drew, T. B., "The Condensation of Mixed Vapors", Transactions of the A.I.Ch.E., 33, p. 197, (1937).
32. Reid, W. T., The Mechanism of Corrosion by Fuel Impurities, Elsevier, New York, (1971).
33. Friedlander, S. K., and Johnstone, H. F., "Deposition of Suspended Particles from Turbulent Gas Streams", Industrial and Engineering Chemistry, 42-7, p. 1151, (1957).
34. Dalmon, J., Tidy, D., and Towell, D. E., "A Surface Sampler for Measuring Solids and Acid Deposition into the Flue-Duct Walls of Oil-Fired Boilers: The CERL Deposition Sampler", Journal of the Institute of Fuel, p. 202, (December 1978).
35. Whittingham, G., "The Influence of Carbon Smokes on the Dew-Point and Sulphur Trioxide Content of Flame Gases", Journal of Applied Chemistry, p. 382, (September 1951).
36. Kear, R. W., "The Influence of Carbon Smokes on the Corrosion of Metal Surfaces Exposed to Flue Gases Containing Sulphur Trioxide", Journal of Applied Chemistry, p. 393, (September 1951).
37. Corbett, P. F., and Flint, D., "The Influence of Certain Smokes and Dusts on the SO<sub>3</sub> Content of the Flue Gases in Power-Station Boilers", Journal of the Institute of Fuel, p. 410, (May 1951).